nature biotechnology

A light- and calcium-gated transcription factor for imaging and manipulating activated neurons

Wenjing Wang[1,2], Craig P Wildes[3], Tanyaporn Pattarabanjird[2], Mateo I Sanchez[1,2], Gordon F Glober[3], Gillian A Matthews[3], Kay M Tye[3] & Alice Y Ting[1,2]

Activity remodels neurons, altering their molecular, structural, and electrical characteristics. To enable the selective characterization and manipulation of these neurons, we present FLARE, an engineered transcription factor that drives expression of fluorescent proteins, opsins, and other genetically encoded tools only in the subset of neurons that experienced activity during a user-defined time window. FLARE senses the coincidence of elevated cytosolic calcium and externally applied blue light, which together produce translocation of a membrane-anchored transcription factor to the nucleus to drive expression of any transgene. In cultured rat neurons, FLARE gives a light-to-dark signal ratio of 120 and a high- to low-calcium signal ratio of 10 after 10 min of stimulation. Opsin expression permitted functional manipulation of FLARE-marked neurons. In adult mice, FLARE also gave light- and motor-activity-dependent transcription in the cortex. Due to its modular design, minute-scale temporal resolution, and minimal dark-state leak, FLARE should be useful for the study of activity-dependent processes in neurons and other cells that signal with calcium.

Neuronal activity is tightly coupled to rises in cytosolic calcium, both in distal dendrites and in the cell body of neurons. Consequently, an important class of tools for studying neuronal activity is real-time fluorescence calcium indicators, including the GCaMP series[1–3] and small-molecule dyes such as Fura-2 (ref. 4) and Fluo-4 (ref. 5). However, these tools have two important limitations. First, real-time imaging is both technically demanding and restricted to small fields of view, should one desire single-cell resolution. Second, these indicators allow one to only passively observe calcium patterns, but not to respond to them—for example, to selectively manipulate or further characterize subsets of neurons based on their history of activity.

A recently reported tool, CaMPARI, addresses the first limitation[6]. CaMPARI is a calcium- and light-gated photoswitchable fluorescent protein. Upon coincident detection of both elevated calcium and violet light, CaMPARI stably converts from a green-emitter to a red-emitter. In contrast to real-time calcium indicators, CaMPARI allows one to integrate the history of calcium elevations in single neurons during time windows defined by the violet light. Subsequently, one can fix the cells or tissue and slowly acquire high-resolution, single-cell data across the entire sample. However, CaMPARI does not address the second limitation, because it provides only a color readout. A more general solution would couple coincident detection of elevated calcium and light in a living cell to transcription of any reporter gene of interest, whether a fluorescent protein, a toxin to ablate neuronal activity, or an opsin to permit subsequent light control of neuronal activity. Furthermore, to improve upon the characteristics of CaMPARI, a new tool would ideally offer light-gating outside of UV wavelengths, which is toxic to cells.

We designed a light-and-calcium-gated transcription factor (TF) system, called FLARE (for Fast Light- and Activity-Regulated Expression; **Fig. 1a**). In the basal state, the TF is tethered to the cell's plasma membrane, unable to activate transcription of the reporter gene located in the cell's nucleus. Upon exposure to both blue light and high calcium, however, the TF is cleaved from the membrane and translocates to the nucleus because (1) the protease recognition site is unblocked by the light-sensitive light-oxygen-voltage sensing (LOV) domain[7,8], and (2) the protease is recruited to its recognition site via a calcium-regulated intermolecular interaction between calmodulin (CaM) and a CaM-binding peptide. High calcium alone is not sufficient to release TF because the protease site remains blocked, and light alone is not sufficient because the protease is far away, and its affinity for its recognition site is too low to give substantial cleavage in the absence of induced proximity. Also key to this design is that both calcium sensing and light sensing are fully reversible, such that sequential rather than coincident inputs (such as high calcium followed by light) are unable to trigger TF release.

The calcium-sensing mechanism of FLARE resembles the protein-proximity-sensing mechanism of Tango[9,10], a tool developed for visualization of G-protein coupled receptor activity. Tango utilizes the tobacco etch virus (TEV) protease (TEVp), which is appealing for its high sequence-specificity; in mammalian cells, TEVp does not recognize and cleave any endogenous proteins. For our initial FLARE constructs, we thus used the TEVp/TEVp cleavage site (TEVcs) pair from Tango. However, these constructs showed no detectable difference in fluorescent protein expression after transient exposure of HEK 293T cells to ionomycin-induced high-calcium conditions (**Fig. 1b**).

Inspection of the images indicated a problem with high background in the low-calcium (untreated) cells. Expression levels of tool

[1]Departments of Genetics, Biology, and Chemistry, Stanford University, Stanford, California, USA. [2]Department of Chemistry, Massachusetts Institute of Technology, Cambridge, Massachusetts, USA. [3]Picower Institute for Learning and Memory and Department of Brain and Cognitive Sciences, Massachusetts Institute of Technology, Cambridge, Massachusetts, USA. Correspondence should be addressed to A.Y.T. (ayting@stanford.edu) or K.M.T. (kaytye@mit.edu).

Received 16 November 2016; accepted 22 May 2017; published online 26 June 2017; doi:10.1038/nbt.3909

components in HEK cells could reach 250 μM or more, exceeding the K_m of the Tango TEVp/TEVcs pair (240 μM (ref. 11)). This would explain the high extent of TEVcs cleavage even in the absence of calcium-induced proximity. C-terminally truncated TEVp has reduced affinity for TEVcs sequences (K_m ~ 450 μM), with minimal reduction in k_{cat}[12] (**Supplementary Fig. 1**). We thus tested truncated TEVp in FLARE, along with two different TEVcs sequences (higher affinity and lower affinity) and three alternative CaMbp sequences (**Fig. 1b**,**c**). As expected, truncated TEVp reduced background signal overall, enabling us to observe a difference in fluorescent protein expression between calcium-treated and untreated cells. Of the three CaMbps tested, M2 gave the lowest background signal.

For light-gating of FLARE, we selected the LOV domain because it has been used *in vivo*[13], is reversible[14], and does not require addition of exogenous cofactors as the Phy-PIF system does[15]. To test light-gating, we fused the LOV2 domain from *Avena sativa*[7] to two TEVcs sequences, truncating the LOV2's C-terminal Jα helix by 2, 3, or 6 amino acids (**Fig. 1d**,**e**). Of six constructs tested, the best one gave only a light-to-dark signal ratio of 2 and dark-state expression was high for all LOV2 fusions (**Fig. 1f**).

For FLARE to be a useful tool, it is imperative to minimize dark-state leak. FLARE will be expressed in cells for days or even weeks before the experiment of interest. During this time, the cells may experience many calcium rises, but we require negligible TF release. Subsequently, a short period of light irradiation permits TF release, if calcium is also elevated at the same time. The large difference in duration between the dark period (days to weeks) and the light-exposure period (min) necessitates a very large light-to-dark signal ratio for FLARE. We found that this was not possible to achieve with the published LOV2 protein (G528A/N538E mutant[7]).

We thus turned to directed evolution to improve the light-caging efficiency of LOV for the TEVcs sequence. We reasoned that specific mutations in LOV2 might enhance the interactions between LOV2 and C-terminally fused TEVcs in the dark state, leading to better steric protection and minimal cleavage by TEV protease in the dark. To implement the evolution (**Fig. 2a**), we mutagenized LOV2 (G528A/N538E mutant[7]) by error-prone PCR, fused it to the TEVcs, and displayed the mutant library on the yeast cell surface via fusion to the Aga2p mating protein. To perform positive selections for efficient TEVcs cleavage in the presence of blue light, we incubated the yeast library with purified TEVp for 1 h under a light source. After staining with antibody–fluorophore conjugates, we used fluorescence-activated cell sorting (FACS) to enrich yeast cells displaying low anti-FLAG/anti-hemagglutinin (HA) fluorescence intensity ratios, indicative of TEVcs cleavage. Negative selections for resistance to TEVp cleavage in the dark were implemented by incubating the yeast library with purified TEV protease in the dark for 3 h, then using FACS to enrich cells with high anti-FLAG/anti-HA fluorescence intensity ratios, indicative of intact TEVcs. We performed six rounds of alternating positive and negative selections (**Supplementary Fig. 2**). These gradually enriched the yeast population displaying LOV mutants with both high TEVcs cleavage in the light state (yellow bars, **Fig. 2b**) and low TEVcs cleavage in the dark state (gray bars, **Fig. 2b**).

Sequencing of enriched clones from round 6 (**Supplementary Fig. 3**) identified five mutants of interest, three of which were superior to the original LOV2 (G528A/N538E mutant[7]) on the yeast surface (**Supplementary Fig. 4a**). We manually combined mutations present in these clones into a single LOV gene to create "eLOV," for evolved LOV (**Supplementary Fig. 4b**,**c**). On the yeast surface (**Fig. 2c**) and in HEK mammalian cells (**Fig. 2d** and **Supplementary Fig. 5**), eLOV was clearly superior to the original LOV2 mutant for light-gating of the TEVcs, especially in the dark state, where Citrine expression resulting from TEVcs cleavage was now minimal. The quantified light-to-dark signal ratio in HEK was 23, in contrast to 2 for the original LOV2 mutant under identical conditions. As anticipated, the introduction of light gating also improved the calcium response of the tool, by reducing the time window for possible accumulation of background signal. The same modules (truncated TEVp, M2 CaMbp) that gave a high-to-low Ca^{2+} signal ratio of only 2 in HEK (**Fig. 1c**) now gave a signal ratio of 16 with eLOV incorporated (signal ratio = 5 with original LOV2 incorporated) (**Fig. 2d**).

The five eLOV mutations discovered via directed evolution are highlighted in **Figure 1d**. Leu2, located in a flexible loop, is mutated to Arg in eLOV. Perhaps this causes the formation of a salt bridge with the Glu sidechain in TEVcs (ENLYFQ▲Y), leading to tighter dark-state caging. H117 is located in the loop that connects the Jα helix to the rest of the LOV domain. H117R in eLOV could potentially stabilize Jα in the dark state by forming a salt bridge to E123 (**Supplementary Fig. 4c**).

We proceeded to test FLARE in the more challenging environment of neurons. Calcium increases in neurons are much more dynamic than the sustained 5-min calcium rises we artificially induced with ionomycin in HEK cells, and cell surface proteins that traffic well in HEK frequently fail to do so in neurons. To address these and other challenges in transitioning FLARE from HEK to neurons, we made a number of changes and improvements to the tool as follows (**Fig. 3a**). First, we expanded our testing of TEVcs sequences (**Supplementary Fig. 6**). Second, we replaced the CD4 segment of FLARE with a neurexin-3β-derived transmembrane domain, which is half the size of CD4 and facilitates packaging into adeno-associated viruses (AAVs). Third, we replaced Gal4 with the tTA-VP16 transcription factor, which has subnanomolar DNA binding affinity and a stronger transcriptional activation domain[16]. Fourth, to facilitate the translocation of cleaved TF from the plasma membrane to the nucleus, we inserted a soma targeting sequence into FLARE. These modifications all contributed to improved FLARE performance in neuron culture (**Fig. 3b**).

Figure 3c,**d** show imaging of our optimized FLARE tool in cultured rat neurons at 19–20 days in vitro (DIV19–20; complete FLARE sequences shown in **Supplementary Fig. 7**). The tTA-VP16 transcription factor drives expression of TRE-mCherry in the nucleus. We stimulated neurons with light for 10 or 15 min using 467-nm blue light at 60 mW/cm^2 and 10–33% duty cycle. To elevate intracellular calcium, we used either electrical stimulation (**Fig. 3d**), or we replaced half of the culture media with fresh media of the same composition (**Fig. 3c**); **Supplementary Figure 8** shows that this latter treatment raises cytosolic calcium. We then allowed neurons 18 h after calcium and light stimulation to transcribe and translate mCherry. mCherry expression was robust only in one of four conditions in each experiment, when neurons were subjected to both light and calcium stimuli (**Fig. 3c**,**d**). There was some detectable background in the light-exposed/low calcium cells (>10-fold less than in the high calcium condition) but this may reflect basal calcium activity (**Supplementary Fig. 8**), as we did not repress or silence these neurons. Notably, mCherry expression was negligible in all dark-state conditions, attesting to the effectiveness of eLOV in caging TEVcs from protease cleavage over the entire 7-d expression window (light-to-dark signal ratios of 121 and 17, respectively; **Fig. 3c**,**d**).

To characterize the sensitivity of FLARE, or the amount of neural activity required to give a reasonable fold-change in transcriptional output we delivered light to neurons for various lengths of time, coincident with two forms of activity stimulation (electrical stimulation or media

change) (**Fig. 3e** and **Supplementary Fig. 9**). Media change produced a robust expression increase (tenfold) in just 4 min, whereas electrical stimulation (at 20 Hz) produced an 11-fold expression increase after 8 min.

The temporal resolution of FLARE is governed by the speed at which FLARE turns on and off. According to previous, the LOV domain and intermolecular CaM-CaMbp interaction both turn on in 1 s or less[17,18]. We measured the reversion kinetics of eLOV, or the rate at which

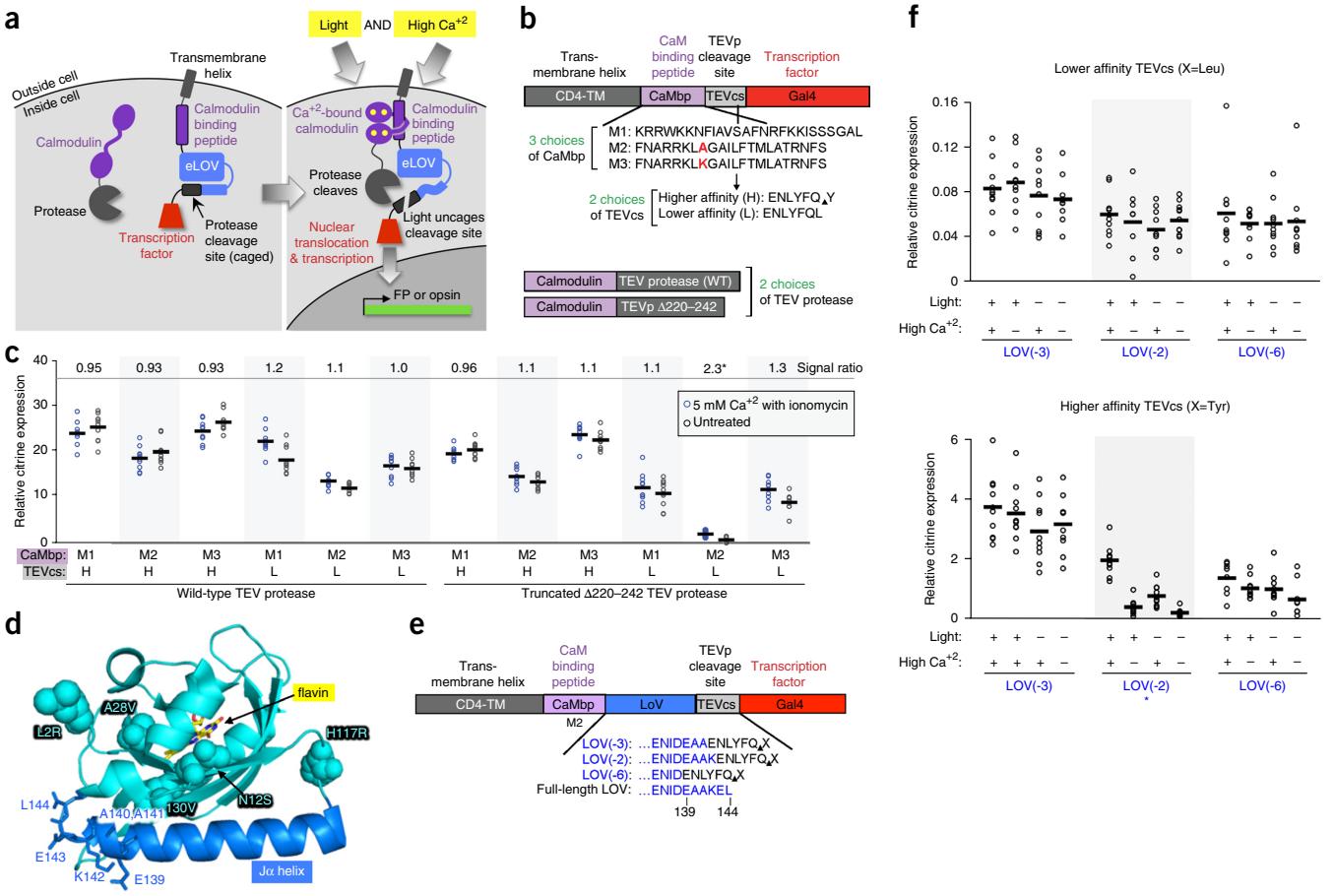

Figure 1 Engineering the calcium and light responses of FLARE. (**a**) FLARE scheme. FLARE components in the dark, low Ca^{+2} state (left) and in the light-exposed, high Ca^{+2} state (right). The evolved LOV domain (eLOV) undergoes a reversible conformational change upon blue light exposure that allows steric access to an adjoining peptide[7,8], in this case, a protease recognition sequence. On the left, the transcription factor (red) is tethered to the plasma membrane, sequestered from the cell nucleus. On the right, the coincidence of neuronal activity (which leads to rises in cytosolic calcium) and blue light causes eLOV to 'uncage' the protease cleavage site, and brings the protease into proximity of its cleavage site, via the intermolecular calmodulin-calmodulin binding peptide interaction. Consequently, the transcription factor is irreversibly cleaved from the plasma membrane, translocates to the nucleus, and activates transcription of the reporter gene of interest. FP, fluorescent protein. (**b**) Summary of constructs tested to optimize the calcium response. None of these contain the light-sensitive LOV/eLOV domain, which is introduced later. For testing in HEK cells, we used Gal4 as the transcription factor and the transmembrane domain of CD4 (ref. 33) to target it to the plasma membrane. We tested three different calmodulin (CaM) binding peptides (CaMbp), two different TEV protease (TEVp) cleavage sites (TEVcs), and two different forms of TEV protease (wild-type and C terminally truncated). For the CaMbps, M1 is the M13 peptide with an A14F 'bump' mutation[34] that complements the 'hole' mutations in our CaM sequence (F19L/V35G, which reduce CaM affinity for endogenous CaM effectors[34]). M2 and M3 CaMbps are derived from CaMKII and reported to have reduced CaM affinities in the low-calcium state[16–18]. For TEVcs, the lower affinity sequence is derived from Tango[9], with a K_m of 240 μM and k_{cat} 0.84 min^{-1}, and the higher affinity sequence has a K_m of 50 μM and k_{cat} of 1.9 min^{-1} (ref. 14). (**c**) Results from testing constructs in **b** in 12 combinations, under low- and high-calcium conditions in HEK cells. Gal4 transcription factor drove the expression of Citrine fluorescent protein, whose intensity was quantified by microscopy in 8–10 fields of view per condition (>250 cells per field of view). To elevate cytosolic calcium, HEK were treated with 5 mM $CaCl_2$ in the presence of 2 μM ionomycin for 5 min; cells were then returned to regular media and Citrine was imaged 12 h later. Signal ratios at top are the ratios of mean Citrine intensities (black horizontal lines) under high versus low-calcium conditions. This experiment has been replicated once. (**d**) Crystal structure of 16 kD *Avena sativa* LOV2 domain (PDB: 2V1A[35]), the basis of FLARE's light gate. Structure in the dark state is shown. Upon blue light irradiation, the bound flavin of LOV2 rapidly (<1 s) conjugates to Cys48, leading to a conformational change that unwinds the C-terminal Jα helix. This results in increased steric access to peptides fused to the C-terminal end of Jα[23]. For FLARE engineering, the residues shown as dark blue sticks at the C-terminal end of Jα were targeted for replacement by the TEV cleavage site ("biting back"). This structure also highlights the mutations we discovered via directed evolution of the LOV domain (**Fig. 2**). The five mutations in evolved LOV (eLOV) are rendered in cyan space-filling mode. (**e**) Summary of LOV-TEVcs fusions tested in FLARE (X in TEVcs = Y or L). LOV here is the published AsLOV2 mutant (G528A/N538E)[7], not our eLOV. (**f**) Results from testing six LOV-TEVcs fusion constructs in HEK cells. Each construct was tested under four conditions and Citrine expression was quantified as in **c**. Calcium was elevated by 5 min $CaCl_2$ and ionomycin treatment as in **c**. Light treatment was 5 min of 467-nm blue light at 60 mW/cm^2, 33% duty cycle (2 s light every 6 s). A star marks the fusion construct with the best performance in this assay (LOV(-2) fused to higher affinity TEVcs). Black horizontal bars are mean values. This experiment has been replicated once.

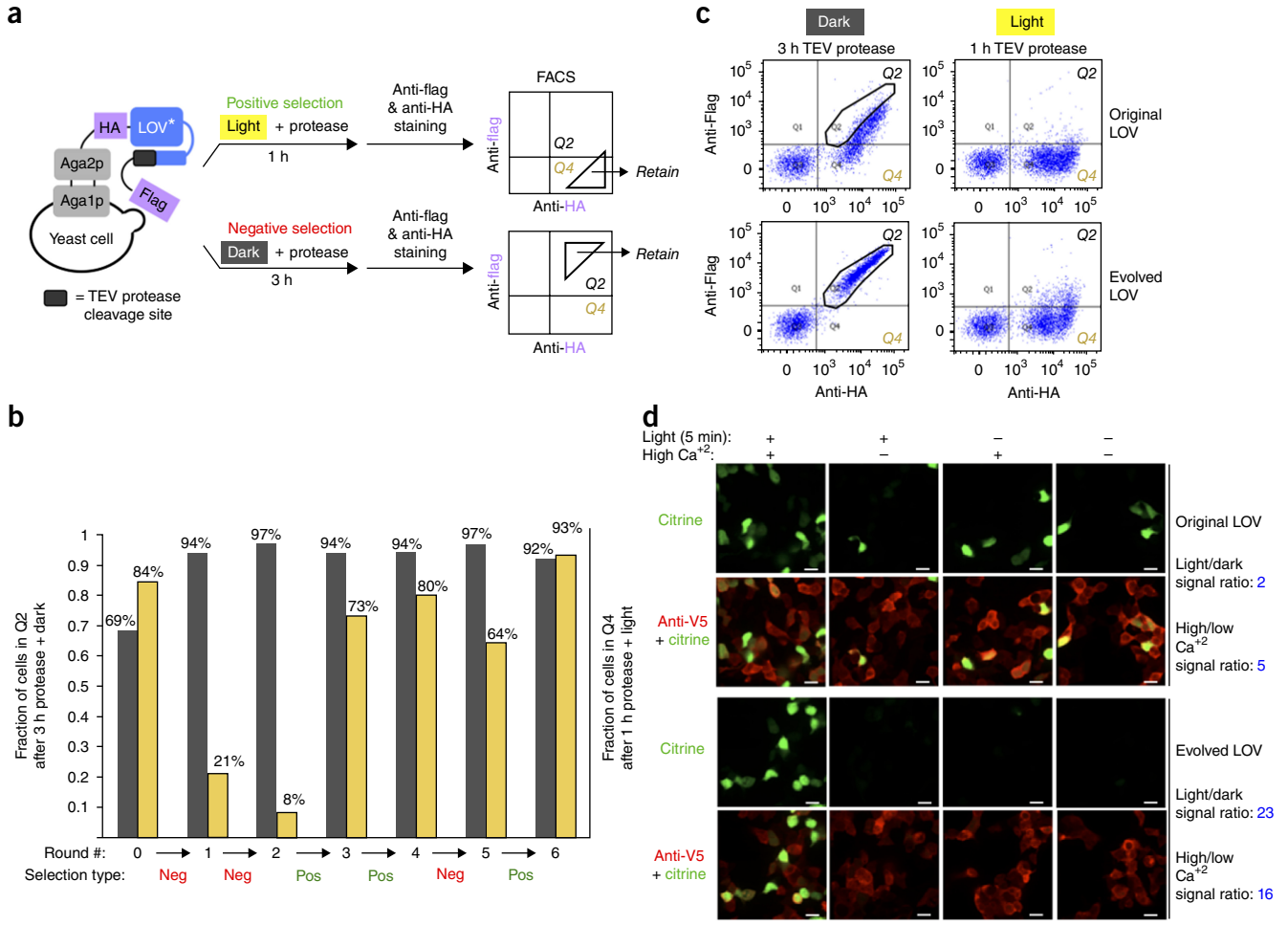

Figure 2 Directed evolution of LOV domain to improve light gating in FLARE. (**a**) Selection scheme. A library of >10^7AsLOV2 variants was displayed on the yeast surface as a fusion to Aga2p protein. The TEVp cleavage site ENLYFQ▲Y (higher affinity) was fused to LOV's C-terminal end, and HA and FLAG are flanking epitope tags. The positive selection (green) enriches mutants with low FLAG staining (i.e., high TEVcs cleavage) after protease treatment in the light. The negative selection (red) enriches mutants with high FLAG staining (i.e., low TEVcs cleavage) after prolonged protease treatment in the dark. (**b**) Graph summarizing yeast library characteristics after each round of selection. (Accompanying FACS plots in **Supplementary Fig. 2**.) Gray bars indicate the fraction of yeast cells in quadrant Q2 (out of all cells in Q2 + Q4) after 3 h of TEV protease incubation in the dark. Quadrants are defined in **a**. Yellow bars indicate the fraction of yeast cells in Q4 (out of all cells in Q2 + Q4) after 1 h of TEV protease incubation in blue light. This experiment was performed once. (**c**) FACS analysis of original AsLOV2 (ref. 7) (top) and our evolved eLOV (bottom) on yeast. eLOV provides superior protection of TEVcs against TEVp cleavage in the dark state (left). eLOV has five mutations relative to AsLOV2 (G528A/N538E mutant[7]; **Fig 1d**). This experiment has been replicated 2 times. (**d**) Comparison of original AsLOV2 (G528A/N538E mutant[7], top) and our evolved eLOV (bottom) in HEK cells, in the context of FLARE. Constructs were TM(CD4)-CaMbp(M2)-(e)LOV-TEVcs(high affinity)-Gal4 and CaM-TEVp(truncated). Gal4 drives expression of the fluorescent protein Citrine. High calcium (5 min) and light conditions were the same as in **Figure 1f**. Anti-V5 staining detects expression of CaM-TEVp. Signal ratios on right are based on mean Citrine intensities across >500 cells from ten fields of view per condition. Scale bars, 20 µm. This experiment has been replicated 2 times.

light-activated eLOV re-sets to the dark state. The reversion time constant was 140 s, similar to the time constants of original LOV2 (G528A/N538E mutant[7]) and WT-LOV2 (ref. 19) (**Supplementary Fig. 10**).

To measure the overall off-rate of FLARE, we staggered light and calcium inputs by various time intervals. If activated eLOV required many minutes to reset to the dark state, then blue light stimulation followed by electrical stimulation would still produce mCherry expression, because the TEVcs would remain accessible for some time after the blue light was removed. Even with an interval as short as 1 min separating light and calcium inputs, mCherry expression was not detectable (**Fig. 3f**). This demonstrates that eLOV reversed to the dark state in less than 1 min, before the subsequent light stimulus was applied. Similarly, calcium followed by light, with only a 1-min intervening gap, produced no mCherry expression. Based on these observations, we conclude that the temporal resolution of FLARE is 1 min or less.

To test if FLARE works by the mechanism that we designed, we imaged neurons using FLARE components containing targeted mutations. Mutations in the calcium binding EF hands of calmodulin, or deletion of the M2 CaMbp from the TF component of FLARE, or mutation of eLOV to remove the cysteine that crosslinks with flavin (C48A) all abolished mCherry expression in the light+ activity condition (**Fig. 3g**).

We tested whether FLARE could be used for functional re-activation of selected neurons (**Fig. 4a**). Instead of driving mCherry expression, we used FLARE to drive expression of a light-activated ion channel, ChrimsonR (a red-shifted depolarizing opsin[20]), fused to mCherry, in neurons exposed to both blue light and electrical stimulation.

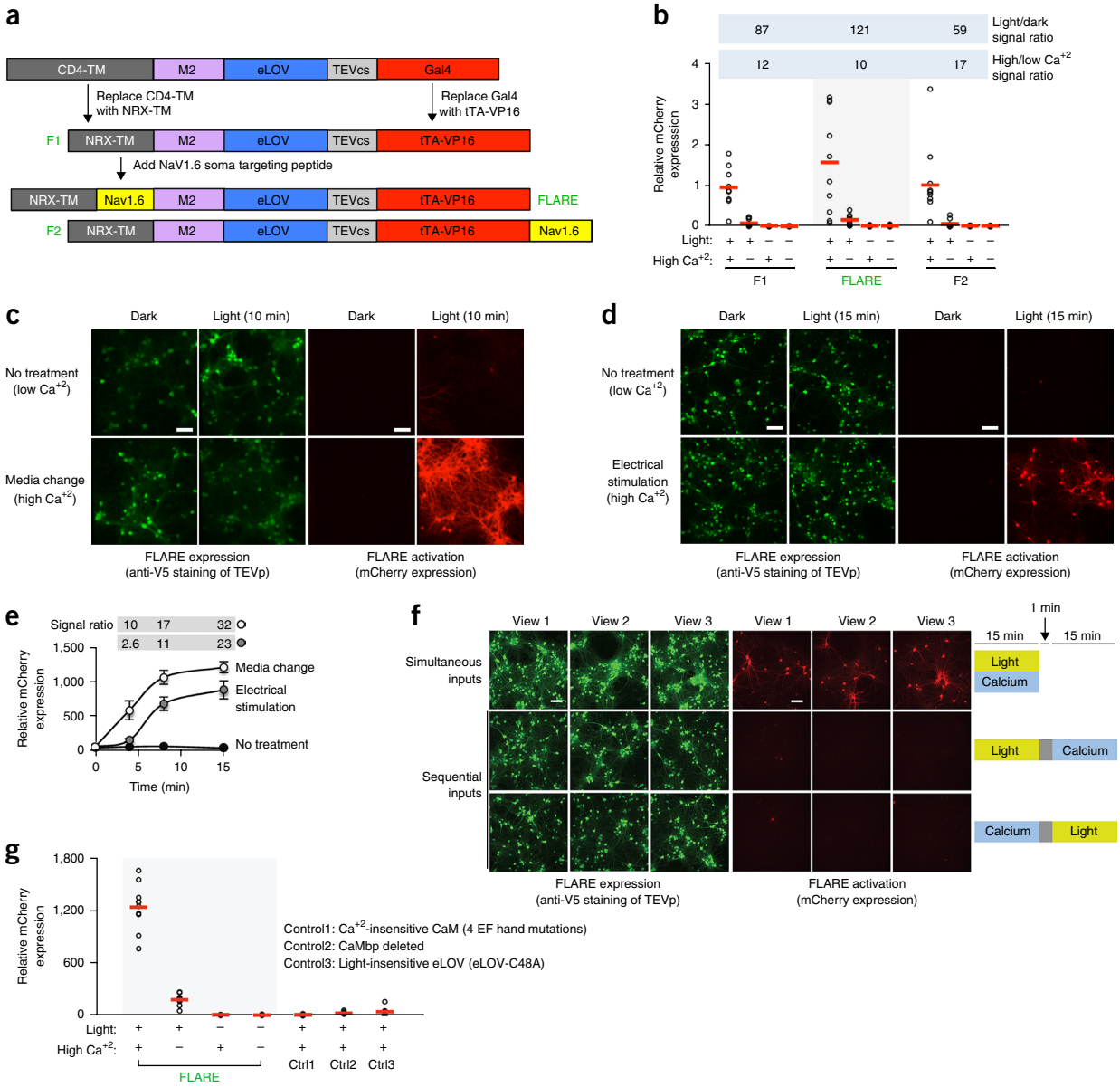

Figure 3 FLARE optimization and testing in neurons. (**a**) Summary of sequential improvements and changes to FLARE. F1 and F2 are earlier versions of the tool. Complete sequences of FLARE components in **Supplementary Figure 7**. (**b**) Comparison of tool versions in neurons. tTA transcription factor drives expression of mCherry. To elevate cytosolic calcium, half of the culture medium was replaced with fresh neurobasal media (of identical composition), and mixed by gentle pipetting. GCaMP5f imaging showed that this treatment produced calcium transients for 10 min or more (**Supplementary Fig. 8**). Low calcium samples were not treated. Light stimulation was for 10 min using 467-nm light at 60 mW/cm^2, 33% duty cycle (2 s light every 6 s). Each data point corresponds to a single field of view with >40 neurons. Red bars denote mean values. This experiment was performed once. (**c**) Confocal imaging of FLARE tool in rat cortical neuron cultures at 20 d *in vitro* (DIV20). Constructs were introduced by AAV viral transduction at DIV13. Calcium and light conditions were identical to those in **b**. 18 h after treatment, neurons were fixed, stained with anti-V5 antibody (to visualize CaM-TEVp expression), and imaged. Quantification shows that the light-to-dark signal ratio is 121, and the high- to low-calcium signal ratio is 10. This experiment has been replicated five times. (**d**) Confocal imaging of FLARE tool after electrical stimulation. Neurons were transduced with AAVs at DIV12 and imaged at DIV19. Electrical stimulation parameters were 3-s trains consisting of 32 1-ms 50 mA pulses at 20 Hz for a total of 15 min. Light was co-applied for 15 min at 467 nm, 60 mW/cm^2, 10% duty cycle (0.5 s every 5 s). Neurons were fixed, stained, and imaged 18 h later. Quantification shows that the light-to-dark signal ratio is 17, and the high- to low-calcium signal ratio is 23. This experiment has been replicated 3 times. (**e**) FLARE sensitivity/time course. DIV18 neurons expressing FLARE were untreated, or activated by electrical stimulation (same parameters as in **d**) or media change (90% of culture medium replaced) for 4, 8, or 15 min with simultaneous application of blue light (467 nm, 60 mW/cm^2, 10% duty cycle (0.5 s light every 5 s)). Signal ratios above reflect mean mCherry intensity ratios with versus without neuronal activity, across ten fields of view per condition. **Supplementary Figure 9** shows a repeat of the media change time course, with additional time points and accompanying fluorescence images. Errors, s.e.m. This experiment has been performed 2 times with the media change protocol and once with the electrical stimulation protocol. (**f**) FLARE is highly specific for simultaneous (top row) rather than sequential (middle and bottom rows) light and calcium inputs. DIV10 cortical neurons expressing FLARE components were activated by electrical stimulation and blue light (same conditions as in **d**). In the case of sequential inputs, a 1-min pause (to allow reversal of eLOV or calcium-sensing domains) separated the two inputs. Three separate fields of view are shown per condition. This experiment has been replicated once. (**g**) Mutagenesis experiments to probe FLARE mechanism. Conditions were the same as in **b**. Control constructs contain mutations in calcium binding, CaM-binding, and light sensitive regions, as described. Red bars denote mean values. This experiment has been replicated once. All scale bars, 100 µm.

With a short, 15-minute single-session stimulation, would resulting opsin expression levels be sufficient to enable functional reactivation of FLARE-marked neurons? Recording of GCaMP5f fluorescence in response to pulses of opsin-activating red light shows that FLARE-marked neurons can indeed be re-activated to give calcium transients (**Fig. 4b**).

To test the potential utility of FLARE for *in vivo* applications, we injected AAV viruses encoding FLARE components into the motor cortex

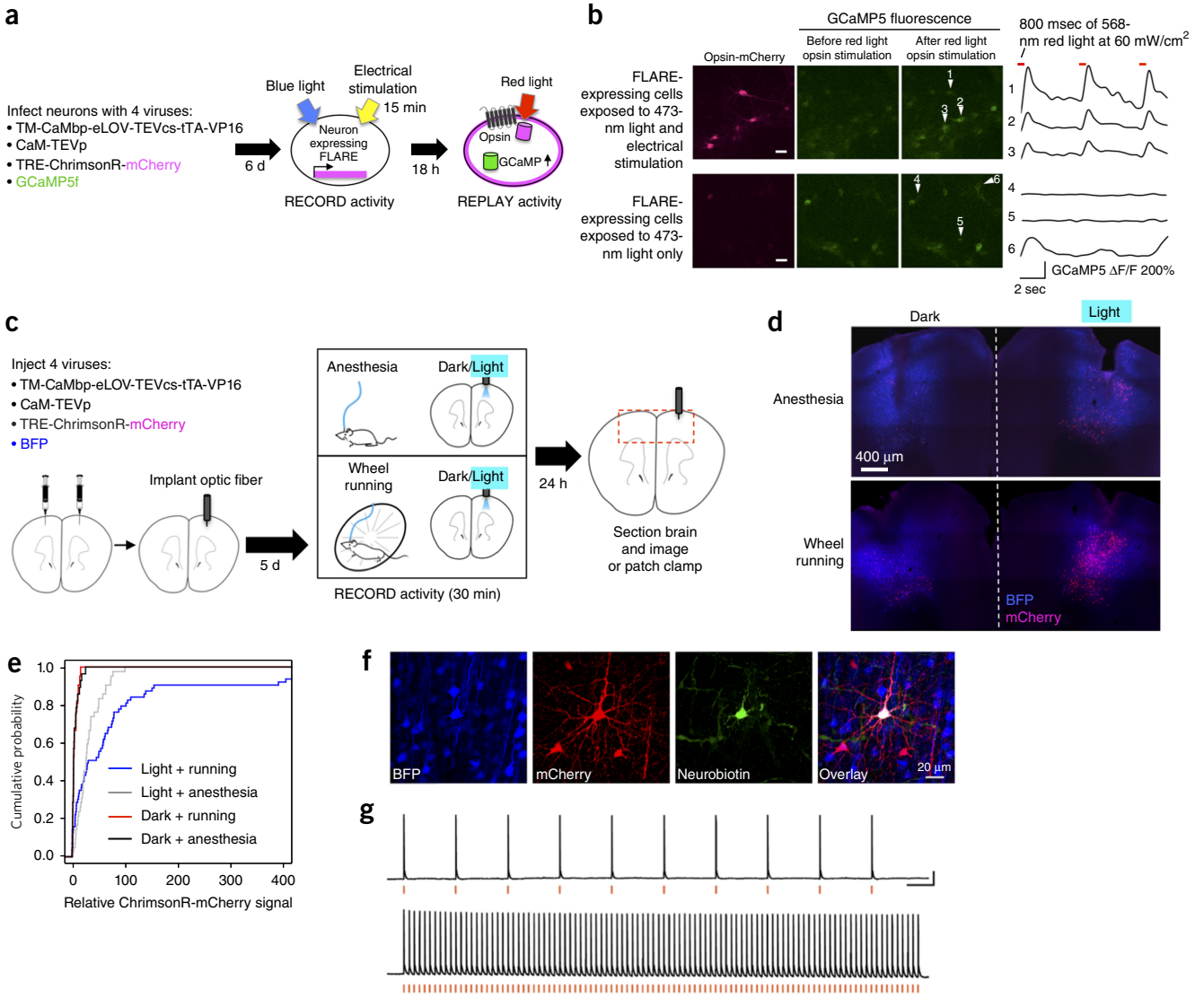

Figure 4 Functional reactivation of neurons marked by FLARE and *in vivo* testing. (**a**) Scheme for activity 'replay' in neuron culture. The coincidence of blue light and high calcium activate FLARE, resulting in expression of opsin(ChrimsonR)-mCherry in subsets of neurons. To re-activate FLARE-marked neurons, red light is applied to stimulate opsin, resulting in cytosolic calcium rises, which can be detected with the GCaMP5f real-time fluorescence calcium indicator[2]. (**b**) Imaging results from experiment performed as in **a**. Cultured rat neurons were transduced with FLARE AAV viruses and GCaMP5f lentivirus at DIV13. At DIV19, neurons were treated with blue light (467 nm at 60 mW/cm^2, 10% duty cycle (0.5 s light every 5 s)) and electrical stimulation (15 min of 3-s long trains, each consisting of 32 1-ms 48 mA pulses at 20 Hz) for 15 min total. 18 h later, at DIV20, GCaMP5f fluorescence time courses were recorded (for the six indicated cells) while stimulating the ChrimsonR opsin with pulses of red 568-nm light as indicated. The bottom image set shows a negative control in which electrical stimulation was withheld at DIV13, but blue light was applied. This experiment has been replicated once. Scale bars, 50 µm. (**c**) Scheme for testing FLARE in the mouse brain. Concentrated AAV viruses encoding FLARE components (in addition to BFP, an infection marker), were injected into the motor cortex of adult mice (both left and right hemispheres, as shown). After 5 d of expression, blue light was delivered to the right hemisphere via implanted optical fiber (single 30-min session of 473-nm light at 0.5 mW, 50% duty cycle (2 s light every 4 s)), while mice were running on an exercise wheel or anesthetized. 24 h later, mice were perfused for imaging analysis. (**d**) Two representative brain sections from experiment in **c**, for anesthetized mouse (top) and wheel running mouse (bottom). Right hemisphere was illuminated for 30 min, whereas left hemisphere was kept in the dark. Activated FLARE drives expression of mCherry. BFP is an AAV infection marker. (**e**) Quantitation of brain imaging data. For each brain hemisphere with BFP signal above background, we quantified the total ChrimsonR-mCherry fluorescence intensity across seven consecutive brain sections around the virus injection site. 21–63 brain sections were analyzed from 3–9 mice per condition. Light + running animals have significantly higher mCherry expression than light + anesthesia animals (Kolmogorov–Smirnov Test, $P = 0.013$). (Alternative presentation of data in **Supplementary Fig. 11). (f**) Whole-cell patch-clamp electrophysiology was used to record from ChrimsonR-mCherry-expressing neurons in the mouse brain 24 h after light + running stimulation. Neurobiotin was injected into the patched neuron. (**g**) Sample traces showing action potentials elicited in response to 5-ms pulses of 589-nm light (red ticks) delivered at 1 Hz (upper panel) or 10 Hz (lower panel). Scale bars = 20 mV, 500 ms. Experiments in **d**–**g** have each been performed once.

of adult mice (**Fig. 4c**). Blue light was delivered via implanted optical fiber, and mice were stimulated via wheel running (single 30-min session) or anesthetized. 24 h later, mice were perfused and imaged for ChrimsonR-mCherry expression to quantify FLARE activation. FLARE was minimally activated in the absence of blue light (**Fig. 4d**,**e** and **Supplementary Fig. 11**). A small but statistically significant ($P = 0.013$) increase in mCherry intensity was observed in animals that were running during the blue light period compared to animals that were inactive (**Fig. 4d**,**e** and **Supplementary Figs. 11** and **12**). To see if FLARE could drive sufficient levels of ChrimsonR expression for functional manipulation, we performed whole-cell patch-clamp recordings from mCherry-positive neurons in the motor cortex of light/running animals, and observed robust red-light-induced action potentials (**Fig. 4f**,**g**). These results suggest that FLARE is gated by light and elevated calcium in the *in vivo* context as well.

A tool that retains memory of past calcium rises has distinct benefits over the real-time calcium indicators that are used ubiquitously in neuroscience. Such a probe integrates calcium activity over user-defined time windows, stores the information in a form that survives cell fixation, and permits the user to carefully survey the entire sample at high resolution. FLARE is such a memory probe, with the additional powerful capability that it can convert calcium memory into transcriptional regulation of any transgene of interest, giving FLARE enormous versatility. In our study, we showed that FLARE-expressing cells exposed simultaneously to blue light and calcium activity for just 10–15 min produced active TFs that drove the expression of EYFP, Citrine, mCherry, or opsin. FLARE can also drive the expression of APEX2, a peroxidase that is useful for electron microscopy[21,22] and live cell proteomic mapping[23] (**Supplementary Fig. 13**). Other transgenes that would be interesting to couple to FLARE include halorhodopsin[24] or tetanus toxin[25] to silence neuronal activity, and DREADDs to regulate neuronal activity with chemical ligands[26].

As the properties of the previously published Tango[9] and LOV[7] modules proved inadequate for attaining high signal-to-noise ratios, we found that it was necessary to engineer improved components. In particular, we truncated the TEV protease and replaced the TEVcs (after screening eight variants) to produce a much more proximity-dependent system with improved calcium gating. For light-gating, we used directed evolution to create eLOV, a light-sensitive protein module that gates the protease-recognition site in FLARE with a light-to-dark signal ratio of >120. Though evolved for one TEVcs sequence in particular, eLOV is more effective than LOV2 (G528A/N538E mutant[7]) at caging a variety of sequences, including recognition sites for other proteases (data not shown). Our study illustrates the power of directed evolution to improve too characteristics, and produces optimized modules that should also be valuable for other protein engineering efforts.

Though promising, our *in vivo* results highlight aspects of FLARE that should be improved to render it a robust and generally applicable tool for circuit mapping in animals. We observe heterogeneity across animals and even across sections from the same animal, because FLARE activity is highly dependent on the expression levels of its components. We delivered FLARE components via viral injection and AAV perfusion through tissue is uneven. Though dark-state leak was negligible in neuron culture, we observed some light-independent background *in vivo* that could be addressed by further engineering of eLOV. Finally, the sensitivity of FLARE is limited by TEV protease turnover rate, which is only 10.8 min^{-1} (and likely much lower for TEVp variants such as split TEVp[27,28]); a faster protease variant could further reduce time windows of tagging. Given the impact that existing "memory trace" tools—that use drug delivery and washout for temporal gating, resulting in tagging time windows of 6–24 h[29–32]—have had on systems neuroscience, a future FLARE tool that works more robustly *in vivo* on the timescale of seconds should provide access to the study and manipulation of a much wider array of cognitive processes.

METHODS

Methods, including statements of data availability and any associated accession codes and references, are available in the online version of the paper.

Note: Any Supplementary Information and Source Data files are available in the online version of the paper.

ACKNOWLEDGMENTS

We thank J. Einstein and A. Draycott for neuron cultures. J. Einstein also assisted with cloning and some imaging assays. F. Zhang, S. Konermann, and M. Brigham provided AAV vectors, AAV protocols, and guided us on the setup of our light stimulation device. G. Liu built the LED light box. M. Heidenreich advised us on preparation of concentrated AAVs. T.J. Wardill and L. Looger provided electrode information. H. Wang and M. Djuristic assisted with electrical stimulation setup. P. Han assisted with statistical analysis of the *in vivo* data. FACS experiments were performed at the Koch Institute Flow Cytometry Core (MIT). The TEVp gene was a gift from the Waugh laboratory (National Cancer Institute). GCaMP5f was a gift from L. Looger, Janelia Research Campus. A.Y.T. received funding from MIT and Stanford. K.M.T. is a New York Stem Cell Foundation Robertson Investigator and McKnight Scholar and this work was supported by funding from the JPB Foundation, the PIIF and PIIF Engineering Award, R01-MH102441-01 (NIMH), and NIH Director's New Innovator Award DP2-DK-102256-01 (NIDDK). G.A.M. was supported by a fellowship from the Charles A. King Trust Postdoctoral Research Fellowship Program, Bank of America, N.A., Co-Trustees.

AUTHOR CONTRIBUTIONS

W.W. performed all experiments except those noted. W.W. and T.P. together performed the LOV directed evolution. M.I.S. generated AAV viruses and measured eLOV recovery kinetics. C.P.W. and K.M.T. designed the *in vivo* experiments. C.P.W., G.F.G., and G.A.M. performed the *in vivo* experiments. W.W. and M.I.S. analyzed the *in vivo* data. W.W. and A.Y.T. designed the research, analyzed the data, and wrote the paper. All authors edited the paper.

COMPETING FINANCIAL INTERESTS

The authors declare competing financial interests: details are available in the online version of the paper.

1. Tian, L. *et al.* Imaging neural activity in worms, flies and mice with improved GCaMP calcium indicators. *Nat. Methods* **6**, 875–881 (2009).
2. Akerboom, J. *et al.* Optimization of a GCaMP calcium indicator for neural activity imaging. *J. Neurosci.* **32**, 13819–13840 (2012).
3. Chen, T.-W. *et al.* Ultrasensitive fluorescent proteins for imaging neuronal activity. *Nature* **499**, 295–300 (2013).
4. Grynkiewicz, G., Poenie, M. & Tsien, R.Y. A new generation of Ca2+ indicators with greatly improved fluorescence properties. *J. Biol. Chem.* **260**, 3440–3450 (1985).
5. Stosiek, C., Garaschuk, O., Holthoff, K. & Konnerth, A. In vivo two-photon calcium imaging of neuronal networks. *Proc. Natl. Acad. Sci. USA* **100**, 7319–7324 (2003).
6. Fosque, B.F. *et al.* Neural circuits. Labeling of active neural circuits in vivo with designed calcium integrators. *Science* **347**, 755–760 (2015).
7. Strickland, D. *et al.* Rationally improving LOV domain-based photoswitches. *Nat. Methods* **7**, 623–626 (2010).
8. Wu, Y.I. *et al.* A genetically encoded photoactivatable Rac controls the motility of living cells. *Nature* **461**, 104–108 (2009).
9. Barnea, G. *et al.* The genetic design of signaling cascades to record receptor activation. *Proc. Natl. Acad. Sci. USA* **105**, 64–69 (2008).
10. Inagaki, H.K. *et al.* Visualizing neuromodulation in vivo: TANGO-mapping of dopamine signaling reveals appetite control of sugar sensing. *Cell* **148**, 583–595 (2012).
11. Kapust, R.B., Tözsér, J., Copeland, T.D. & Waugh, D.S. The P1′ specificity of tobacco etch virus protease. *Biochem. Biophys. Res. Commun.* **294**, 949–955 (2002).
12. Kapust, R.B. *et al.* Tobacco etch virus protease: mechanism of autolysis and rational design of stable mutants with wild-type catalytic proficiency. *Protein Eng.* **14**, 993–1000 (2001).
13. Hayashi-Takagi, A. *et al.* Labelling and optical erasure of synaptic memory traces in the motor cortex. *Nature* **525**, 333–338 (2015).
14. Pudasaini, A., El-Arab, K.K. & Zoltowski, B.D. LOV-based optogenetic devices: light-driven modules to impart photoregulated control of cellular signaling. *Front. Mol. Biosci.* **2**, 18 (2015).

15. Levskaya, A., Weiner, O.D., Lim, W.A. & Voigt, C.A. Spatiotemporal control of cell signalling using a light-switchable protein interaction. *Nature* **461**, 997–1001 (2009).
16. Orth, P., Schnappinger, D., Hillen, W., Saenger, W. & Hinrichs, W. Structural basis of gene regulation by the tetracycline inducible Tet repressor-operator system. *Nat. Struct. Biol.* **7**, 215–219 (2000).
17. Park, H.Y. *et al.* Conformational changes of calmodulin upon Ca2+ binding studied with a microfluidic mixer. *Proc. Natl. Acad. Sci. USA* **105**, 542–547 (2008).
18. Konold, P.E. *et al.* Unfolding of the C-terminal Jα Helix in the LOV2 photoreceptor domain observed by time-resolved vibrational spectroscopy. *J. Phys. Chem. Lett.* **7**, 3472–3476 (2016).
19. Zayner, J.P. & Sosnick, T.R. Factors that control the chemistry of the LOV domain photocycle. *PLoS One* **9**, e87074 (2014).
20. Klapoetke, N.C. *et al.* Independent optical excitation of distinct neural populations. *Nat. Methods* **11**, 338–346 (2014).
21. Martell, J.D. *et al.* Engineered ascorbate peroxidase as a genetically encoded reporter for electron microscopy. *Nat. Biotechnol.* **30**, 1143–1148 (2012).
22. Lam, S.S. *et al.* Directed evolution of APEX2 for electron microscopy and proximity labeling. *Nat. Methods* **12**, 51–54 (2015).
23. Rhee, H.W. *et al.* Proteomic mapping of mitochondria in living cells via spatially restricted enzymatic tagging. *Science* **339**, 1328–1331 (2013).
24. Gradinaru, V. *et al.* Molecular and cellular approaches for diversifying and extending optogenetics. *Cell* **141**, 154–165 (2010).
25. Nakashiba, T., Young, J.Z., McHugh, T.J., Buhl, D.L. & Tonegawa, S. Transgenic inhibition of synaptic transmission reveals role of CA3 output in hippocampal learning. *Science* **319**, 1260–1264 (2008).
26. Armbruster, B.N., Li, X., Pausch, M.H., Herlitze, S. & Roth, B.L. Evolving the lock to fit the key to create a family of G protein-coupled receptors potently activated by an inert ligand. *Proc. Natl. Acad. Sci. USA* **104**, 5163–5168 (2007).
27. Wehr, M.C. *et al.* Monitoring regulated protein-protein interactions using split TEV. *Nat. Methods* **3**, 985–993 (2006).
28. Lee, D. *et al.* Temporally precise labeling and control of neuromodulatory circuits in the mammalian brain. *Nat. Methods* **14**, 495–503 (2017).
29. Liu, X. *et al.* Optogenetic stimulation of a hippocampal engram activates fear memory recall. *Nature* **484**, 381–385 (2012).
30. Guenthner, C.J., Miyamichi, K., Yang, H.H., Heller, H.C. & Luo, L. Permanent genetic access to transiently active neurons via TRAP: targeted recombination in active populations. *Neuron* **78**, 773–784 (2013).
31. Reijmers, L.G., Perkins, B.L., Matsuo, N. & Mayford, M. Localization of a stable neural correlate of associative memory. *Science* **317**, 1230–1233 (2007).
32. Sørensen, A.T. *et al.* A robust activity marking system for exploring active neuronal ensembles. *eLife* **5**, 2 (2016).
33. Feinberg, E.H. *et al.* GFP Reconstitution Across Synaptic Partners (GRASP) defines cell contacts and synapses in living nervous systems. *Neuron* **57**, 353–363 (2008).
34. Palmer, A.E. *et al.* Ca2+ Indicators based on computationally redesigned calmodulin-peptide pairs. *Chem. Biol.* 1**3**, 521–530 (2006).
35. Halavaty, A.S. & Moffat, K. N- and C-terminal flanking regions modulate light-induced signal transduction in the LOV2 domain of the blue light sensor phototropin 1 from Avena sativa. *Biochemistry* **46**, 14001–14009 (2007).

ONLINE METHODS

Cloning. All constructs for protein expression in HEK 293T cells, neuron culture, and the mouse brain were cloned into the pAAV viral vector (a gift from F. Zhang, MIT). For HEK cells, we used the cytomegalovirus (CMV) promoter to drive expression. For neuron culture and mouse brain, we used the synapsin promoter.

All constructs for yeast display were cloned into the pCTCON2 vector. The calcium indicator GCaMP5f was cloned into the lentiviral vector FSW, derived from FUGW, and the promoter was synapsin. TEV protease was cloned into THE pET21b vector for bacterial expression and purification. LOV constructs were cloned into the pYFJ16 vector for bacterial expression and purification.

Supplementary Table 1 lists all 44 plasmids used in this work. The TEV protease gene was a gift from the Waugh laboratory (National Cancer Institute). The calmodulin (CaM) gene was amplified from GCaMP5f, a gift from L. Looger, Janelia Research Campus. AsLOV2 was synthesized via overlap extension PCR.

For cloning, PCR fragments were amplified using Q5 polymerase (New England BioLabs (NEB)). The vectors were double-digested and ligated to gel-purified PCR products by T4 ligation or Gibson assembly. Ligated plasmid products were introduced by heat shock transformation into competent XL1-Blue bacteria.

Expression and purification of TEV protease. Full-length TEV protease (TEVp) was expressed as a fusion to maltose binding protein (MBP), from BL21-CodonPlus(DE3)-RIPL *Escherichia coli* (*E. coli*). Homemade competent BL21 cells were transformed via heat shock with the MBP-TEVp(S219V)-pET21b expression plasmid. Cells were cultured in 50 mL LB (Luria-Bertani, Miller) media with 100 mg/L ampicillin at 37 °C with shaking at 220 r.p.m. overnight. Then 10 mL of this saturated culture was used to inoculate 1 liter LB with 100 mg/L ampicillin, which was grown at 37 °C with 220 r.p.m. shaking until OD_{600} = 0.6. IPTG (isopropyl β-D-1-thiogalactopyranoside, EMD Millipore) was added to the culture to a final concentration of 1 mM, and the culture was transferred to 25 °C for continued shaking at 220 r.p.m. for 12 h. Cells were harvested by centrifugation at 5,000 r.p.m. at 4 °C. Pelleted cells were lysed in ice-cold B-PER buffer (Thermo Fisher Scientific) supplemented with 1 mM DTT (Sigma-Aldrich, freshly made), then clarified by centrifugation at 10,000 r.p.m. for 15 min at 4 °C. The supernatant was incubated with 1 mL of Ni-NTA bead slurry (Thermo Fisher) at 4 °C for 10 min with rotation and then transferred to a gravity column. The beads were washed at 4 °C with 10 mL washing buffer (30 mM imidazole, 50 mM Tris, 300 mM NaCl, 1 mM DTT, pH = 7.8), then protein was eluted with 10 mL elution buffer (200 mM imidazole, 50 mM Tris, 300 mM NaCl, 1 mM DTT, pH = 7.8). The eluents from five separate preparations (five original 1-liter cultures) were combined and concentrated with a 15 mL 10,000 Da cutoff centrifugal unit (Millipore) to OD_{280} ~ 70.

This purified and concentrated TEV protease was used for LOV-directed evolution experiments. To successfully implement the negative selections, we required very active and concentrated TEV protease to achieve appreciable TEVcs cleavage in the dark, LOV-caged state, and in the absence of induced proximity between protease and TEVcs.

We note that TEV protease is sensitive to oxidizing conditions, because it has an active-site cysteine. Purification and storage should all be under reducing conditions. Even with these precautions, we observed a great deal of batch-to-batch variation in TEV protease yield and activity.

Yeast strains, transformation, and cell culture. Yeast expressing HA-LOV-TEVcs-FLAG protein as a fusion to Aga2p surface protein was generated by transformation of *Saccharomyces cerevisiae* strain EBY100-competent cells with the yeast display plasmid pCTCON2 (ref. 36). To generate EBY100-competent cells, an overnight 1-d-old culture of saturated EBY100 cells at OD_{600} > 10 was diluted 10- to 20-fold into 10 mL fresh YPD broth (yeast extract peptone dextrose, 20 g dextrose, 20 g peptone (BD) and 10 g yeast extract (BD) in 1 liter deionized H_2O), to OD_{600} ~ 0.5, and grown at 30 °C with shaking at 220 r.p.m. for 4–6 h until the OD_{600} reached 1.5. The cells were pelleted by centrifugation at 3,000 r.p.m. for 3 min, washed with 10 mL EZ1 solution (Frozen-EZ Yeast Transformation II, Zymo Research), then re-pelleted and resuspended with 1 mL EZ2 solution (Frozen-EZ Yeast Transformation II, Zymo Research). The cell suspension was divided into 20-µL aliquots and frozen slowly at −20 °C and stored at −80 °C.

For transformation of EBY100-competent cells22, 300 ng of pCTCON2 DNA was mixed with 20 µL of thawed EBY100 competent cells, then 500 µL of EZ3 solution (Frozen-EZ Yeast Transformation II, Zymo Research) was added and thoroughly mixed, and the solution was incubated at 30 °C for 45 min. The cells were mixed a few more times during the 45-min period and then plated onto synthetic dextrose plus casein amino acid (SDCAA) plates lacking tryptophan. Colonies of transformed cells containing the *Trp1* gene were selected after 2 d of incubation at 30 °C. Single colonies were used to inoculate 5 mL SDCAA media, which was cultured at 30 °C and 220 r.p.m. for 24 h until OD_{600} > 5. pCTCON2 construct expression was induced by combining 500 µL of the overnight yeast culture with 5 mL of SGCAA (synthetic galactose plus casein amino acid) media, and culturing at 30 °C and 220 r.p.m. for 12–24 h.

Generation of LOV mutant library by error-prone PCR and transformation into yeast. To perform error-prone PCR, we combined 100 ng of the template plasmid (Aga2p-HA-LOV-TEVcs-FLAG in pCTCON2) with 0.4 µM forward and reverse primers that anneal to the sequences just outside the 5′ and 3′ ends of the gene encoding AsLOV2 (sequences below), 2 mM $MgCl_2$, 5 units of Taq polymerase (NEB), 1× Taq polymerase buffer (NEB) and 2 µM each of the mutagenic nucleotide analogs 8-oxo-2′-deoxyguanosine-5′-triphosphate (8-oxo-dGTP) and 2′-deoxy-p-nucleoside-5′-triphosphate (dPTP) in a total volume of 50 µL (two reactions were required).

Forward primer:

5′GCTCTGCAGCAAGGTCTGCAGGCTAGTGGTGGAGGAGGCTCTGGTGCTAGC

Reverse primer:

5′CTTATCGTCGTCATCCTTGTAGTCGGATCCTCCGCCGTACTGGAAGTAGAGATTTTC

The PCR was run for 20 cycles with an annealing temperature of 58 °C per cycle. Then the PCR product was gel-purified, and re-amplified for another 30 cycles with 0.4 µM forward and reverse primers that introduce ~45 bp of overlap with both ends of the vector:

Forward primer:

5′GCTCTGCAGCAAGGTCTGCAGGCTAGTGGTGGAGGAGGCTCTGGTGCTAGC

Reverse primer: 5′CTGTTGTTATCAGATCTCGAGCTATTACTTATCGTCGTCATCCTTGTAGTCGGATCC

PCR annealing temperature was 58 °C and 100 µM regular dNTPs (VWR) and 5 units of Taq polymerase in 50 µL volume were used. The PCR products from four separate reactions were combined and purified by gel extraction.

Separately, we linearized the Aga2p-HA-LOV-TEVcs-FLAG-pCTCON2 plasmid by digesting with BamHI and NheI restriction enzymes for 3 h at 37 °C. These enzymes digest the gene just upstream of the LOV domain and downstream of the TEVcs. The linearized plasmid was purified by gel extraction. We then combined 1 µg of linearized vector with 4 µg of mutagenized LOV PCR product from above, and concentrated using pellet paint (Millipore) according to the manufacturer's protocols. The DNA was precipitated with ethanol and sodium acetate, and resuspended in 10 µL ddH_2O.

In parallel, fresh electrocompetent EBY100 cells were prepared. EBY100 cells were passaged at least two times before this procedure to ensure that the cells were healthy. We used a 2- to 3-mL saturated culture of fresh EBY100 cells to inoculate 100 mL of fresh YPD media, and grew the cells with shaking at 220 r.p.m. at 30 °C for 6–8 h until the OD_{600} reached 1.5–1.8. The cells were then harvested by centrifugation for 3 min at 3,000 r.p.m. and resuspended in 50 mL of sterile 100 mM lithium acetate in water, by vigorous shaking. Fresh sterile DTT (1 M stock solution, made on the same day) was added to the yeast cells to a final concentration of 10 mM. The cells were incubated with shaking at 220 r.p.m. for 12 min at 30 °C (necessary to ensure adequate oxygenation). Then cells were pelleted at 4 °C by centrifugation at 3,000 r.p.m. for 3 min and washed once with 25 mL ice-cold sterile water, pelleted again, and resuspended in 1 mL ice-cold sterile water.

The concentrated mixed DNA from above was combined with 250 µL of electrocompetent EBY100 cells on ice and then electroporated using a Bio-Rad Gene pulser XCell with the following settings: 500-V, 15-ms pulse duration,

one pulse only, 2-mm cuvette. The electroporated cells were immediately rescued with 2 mL pre-warmed YPD media and then incubated at 30 °C for 1 h without shaking. 10 µL of this solution was used to determine transformation efficiency, and the remainder was pelleted to remove the YDP media, and resuspended in 100 mL SDCAA media supplemented with 50 units/mL penicillin and 50 µg/mL streptomycin. The culture was grown at 30 °C with shaking at 220 r.p.m. for 1 d, before induction of protein expression and positive selection as described below ("Yeast display selection").

The transformation efficiency of our LOV library into EBY100 yeast was determined to be 3.6×10^7. DNA sequencing of 12 individual clones (**Supplementary Fig. 3**) showed that each clone had 0–2 nucleotides changed relative to the original AsLOV2 template.

Yeast display selection. EBY100 yeast cells transformed with the LOV library in pCTCON2, as described above ("Generation of LOV mutant library by error prone PCR and transformation into yeast"), were induced by transferring them to 1:10 SDCAA/SGCAA media, and growing the cells for 18–24 h at 30 °C with shaking at 220 r.p.m. For the first round of selection, 1 mL of saturated yeast culture (at OD_{600} ~15; note that OD_{600} ~1 corresponds to roughly 1×10^7 yeast cells/mL) was pelleted in a clear microfuge tube at 5,000 r.p.m. for 2 min. For subsequent rounds of selection (rounds 2–6), 0.5 mL of a saturated culture was pelleted in this way. Pelleted cells were then washed twice with 1 mL PBSB (sterile phosphate-buffered saline supplemented with 0.1% BSA). To remove residual liquid on the walls of the microfuge tube, the cells were pelleted again at 5,000g for 30 s, and any remaining liquid was removed by gentle pipetting. To provide an opportunity for any light-activated LOV protein to reset or return to the dark state, we kept the yeast cells in the dark for at least 5 min before addition of exogenous TEV protease for the positive selection. All subsequent manipulations were performed in a dark room with a red light source to prevent unintended activation of the LOV domain.

To implement the positive selections, we added to the yeast cell pellet purified self-cleavage inhibiting full-length TEV(S219V) protease diluted in PBSB, expressed and purified from *E. coli* as described above ("Expression and purification of TEV protease"), to a final concentration of 30 µM. Cells were resuspended and then placed under a daylight lamp (T5 Circline Fluorescent Lamp, 25W, 6500K, 480 nm/530 nm/590 nm) while under rotation for 1 h at room temperature.

To implement the negative selection, we added the same quantity of purified TEV protease, wrapped the tube in aluminum foil, and rotated for 3 h at room temperature in the dark. Then, yeast cells (from both positive and negative selections) were pelleted by centrifugation (5,000 r.p.m., room temperature, 2 min), washed with room temperature PBSB twice, and labeled with primary antibodies. Sigma mouse-anti-FLAG antibody and Rockland rabbit-anti-HA antibody were each added at 1:200 dilution (**Supplementary Table 2**), and incubated with the cells at room temperature for 30 min with rotation. After washing twice with PBSB, we then labeled with the secondary antibodies anti-mouse-AlexaFluor 647 (Life Technology, 1:200 dilution) and anti-rabbit-phycoerythrin (Invitrogen, 1:200 dilution). The labeled yeast cells were resuspended in PBSB to a concentration of 5×10^7 cells/mL and sorted by FACS into a collection tube with 5 mL SDCAA with 50 units/mL penicillin and 50 µg/mL streptomycin. We used a Beckman Coulter MoFlo sorter with 488-nm and 640-nm lasers and 580/30 (for phycoerythrin) and 657 low-pass (for AlexaFluor647) emission filters.

In total, six rounds of alternating positive and negative selections were performed. Gates were drawn as shown in **Supplementary Figure 2** to collect the following quantities of cells:

Round 1 (negative selection): 0.5% of cells collected (2.8×10^5 cells)
Round 2 (negative selection): 25% of cells collected (1×10^6 cells)
Round 3 (positive selection): 3.5% of cells collected (1.2×10^5 cells)
Round 4 (positive selection): 9.3% of cells collected (5.0×10^5 cells)
Round 5 (negative selection): 1.35% of cells collected (1.2×10^5 cells)
Round 6 (positive selection): 3.1% of cells collected (3.7×10^5 cells)

The collected yeast cells were immediately put to a 30 °C incubator with shaking at 220 r.p.m. Yeast cells were grown until saturation (it takes 1–2 d) and then 500 µL of the yeast culture was added to 5 mL of SGCAA media and culturing at 30 °C and 220 r.p.m. for 12–24 h. Saturated yeast cells (500 µL) were spun down and labeled for the next round of sorting.

FACS analysis. To analyze sorted yeast populations, we prepared saturated overnight cultures for each cell population, then diluted by 1:10 in SGCAA media to induce protein expression. After shaking each 5.5 mL culture at 220 r.p.m. and 30 °C for 12–24 h, we pelleted the cells by centrifugation (5,000 r.p.m. for 2 min at room temperature), washed with PBSB twice, and then re-pelleted. We treated half the sample with purified TEV protease at C_f 30 µM in the dark for 3 h, and half in the light for 1 h. Yeast cells were then labeled with anti-FLAG and anti-HA primary antibodies, then anti-rabbit and anti-mouse secondary antibodies, as described above, before FACS analysis. We used an LSRII flow cytometer (BD Biosciences) to analyze yeast with 488-nm and 640-nm lasers and 582/42 (for phycoerythrin) and 670/30 (for AlexaFluor647) emission filters.

Cloning, expression, and purification of LOV proteins. For *in vitro* characterization of LOV proteins, we cloned the LOV genes into pYFJ16 vector for *E. coli* expression. LOV proteins were fused at their N-terminal ends, via a SGGGGSTGGGSSGG linker, to *E. coli* maltose binding protein (MBP). Competent BL21-CodonPlus(DE3)-RIPL *E. coli* were transformed with LOV expression plasmids by heat shock transformation. Cells were grown in LB media with 100 mg/L ampicillin at 37 °C and 220 r.p.m. until OD_{600} 0.6. Protein expression was then induced with 1 mM (C_f) IPTG, and cultures were grown with shaking at 220 r.p.m. and 18 °C for another 18 h. Bacteria were pelleted by centrifugation at 6,000 r.p.m. for 6 min at room temperature and immediately lysed with B-PER (20 mL per 1 liter of original culture). The lysate was clarified by centrifugation at 10,000 r.p.m. for 15 min at 4 °C and then incubated with Ni-NTA agarose beads (QIAGEN) in binding buffer (50 mM Tris, 300 mM NaCl, pH = 7.8) for 10 min. The slurry was placed in a gravity column and washed with washing buffer (30 mM imidazole, 50 mM Tris, 300 mM NaCl, pH = 7.8). The protein was eluted with elution buffer (200 mM imidazole, 50 mM Tris, 300 mM NaCl, pH = 7.8). Bright yellow protein fractions were collected and transferred to a centrifugal filter Amicon Ultra-15 and exchanged 3 times into ice-cold DPBS (Dulbecco's Phosphate Buffer Saline). Purified LOV proteins were characterized within the same day as their production and purification.

UV-Vis spectroscopy of LOV proteins (Supplementary Fig. 10). We characterized the reversion kinetics of purified LOV proteins, from light state to dark state, following previous procedures[37,38]. UV-Vis spectra were acquired using a Nanodrop2000c spectrophotometer with a 5-nm slit width and a 1-cm path length at 22 °C. Kinetic traces were acquired after photosaturation of freshly purified LOV proteins (~10 µM in DPBS) with MaestroGen UltraBright LED transilluminator (470 nm, 30 s). Absorbance spectra were then acquired on a Nanodrop 2000c Spectrophotometer at 448 nm (λ_{max}) every 2 s for 5 min. The data were fit to a single exponential decay to calculate the lifetime of the LOV light state.

Fluorescence microscopy of cultured cells. Confocal imaging was performed on a Zeiss AxioObserver inverted confocal microscope with 10× air and 40× oil-immersion objectives, outfitted with a Yokogawa spinning disk confocal head, a Quad-band notch dichroic mirror (405/488/568/647), and 405 (diode), 491 (DPSS), 561 (DPSS) and 640-nm (diode) lasers (all 50 mW). The following combinations of laser excitation and emission filters were used for various fluorophores: Citrine/GCaMP/Alexa Fluor 488 (491 laser excitation; 528/38 emission), mCherry/Alexa Fluor 568 (561 laser excitation; 617/73 emission), Alexa Fluor 647 (647 excitation; 680/30 emission), and differential interference contrast (DIC). Acquisition times ranged from 100 to 800 ms. All images were collected and processed using SlideBook (Intelligent Imaging Innovations).

HEK 293T cell culture and transfection. HEK293T cells from ATCC with fewer than 20 passages were cultured as monolayers in complete growth media, DMEM (Dulbecco's Modified Eagle medium, Gibco) supplemented with 10% FBS (Fetal Bovine Serum, Sigma), at 37 °C under 5% CO_2. For imaging at 10× magnification, we grew the cells in plastic 48-well plates that were pretreated with 50 µg/mL human fibronectin (Millipore) for at least 10 min at 37 °C before cell plating (to improve adherence of HEK cells). For imaging at 40× magnification, we grew cells on 7 × 7 mm glass cover slips placed inside 48-well plates. The coverslips were also pretreated with 50 µg/mL human fibronectin

doi:10.1038/nbt.3909

for at least 10 min at 37 °C before cell plating. Cells were transfected at 60–90% confluence with 1 mg/mL PEI max solution (polyethylenimine HCl Max pH 7.3). For transfection of a single well in a 48-well plate, a mix of DNA (15 ng of UAS-Citrine plasmid; 15 ng of FLARE protease plasmid; and 50–100 ng of FLARE TF plasmid) was incubated with 0.8 µL PEI max in 10 µL serum-free DMEM media for 15 min at room temperature. DMEM with 10% FBS (100 µL) was then mixed with the DNA-PEI max solution and added to the HEK 293T cells and incubated for 18 h before further processing.

HEK 293T cell stimulation, imaging, and data analysis for calcium-dependent protease cleavage (Fig. 1c). HEK 293T cells were processed 18 h post-transfection. To elevate cytosolic calcium, 100 µL of ionomycin and $CaCl_2$ in complete growth media was added gently to the top of the media in a 48-well plate to final concentrations of 2 µM and 5 µM, respectively. For low Ca^{2+} conditions, 100 µL complete growth media was added. After a 5-min incubation, the solution in the 48-well plates was removed and the cells were washed once and then incubated with 200 µL complete growth media. Thereafter, HEK cells were incubated for 12 h at 37 °C before fixation with 4% paraformaldehyde in PBS (phosphate buffered saline) for 15 min at room temperature. HEK 293T cells were permeabilized by incubation with cold methanol at −20 °C for 5 min, then immunostained with mouse-anti-V5 antibody (1:2,000 dilution, Life Technology) and rabbit-anti-HA antibody (1:1,000 dilution, Rockland) in 2% BSA solution in PBS for 30 min at room temperature with gentle rocking. The cells were washed twice with room temperature PBS and then incubated with secondary antibodies: anti-mouse-Alexa Fluor 568 (1:1,000 dilution, Life Technology) and anti-rabbit-Alexa Fluor 647 (1:1,000 dilution, Life Technology) in 2% BSA solution in PBS, for 20 min at room temperature. Cells were washed twice with PBS and maintained in PBS at 4 °C until imaging.

HEK 293T cells directly plated into 48-well plates were imaged with the 10× air objective on the Zeiss AxioObserver inverted confocal microscope. Eight to ten fields of view were acquired for each condition. A mask was defined according to anti-V5 immunofluorescence (expression of the FLARE protease component). Within this mask, we calculated the mean Citrine intensity (= Intensity 1). A second mask was drawn in the area outside of V5 immunofluorescence and mean Citrine intensity here was calculated as Intensity 2 (background). Intensity 1 was subtracted by Intensity 2 for each field of view. Background-corrected mean Citrine intensities from 8–10 fields of view were averaged together and reported for each condition (**Fig. 1c**).

HEK 293T cell stimulation, imaging, and data analysis for light- and calcium-dependent protease cleavage (Fig. 1f). HEK 293T cells were maintained in the dark, wrapped in aluminum foil, following transfection with FLARE plasmids. All manipulations were performed in a dark room with red light illumination to prevent unwanted activation of the LOV domain (which is activated by ambient room light). HEK 293T cells were processed 18 h post-transfection. For high Ca^{2+} conditions, 100 µL ionomycin (Sigma-Aldrich) and $CaCl_2$ in complete growth media were added gently to the top of the media in a 48-well plate to final concentrations of 2 µM and 5 µM, respectively. For low Ca^{2+} conditions, 100 µL complete growth media was added. Immediately following Ca^{2+} stimulation, one 48-well plate of HEK 293T cells was placed on top of a custom-built LED light box that delivers 467-nm blue light at 60 mW/cm^2 intensity and 33% duty cycle (2 s of light every 6 s). Cells were irradiated on the blue LED light box for 5 min total. For the dark condition, HEK 293T cells were wrapped in aluminum foil. Afterwards, media in each well was removed, and the cells were washed once and then incubated with 200 µL complete growth media. HEK 293T cells were then incubated in the dark at 37 °C for 12 h more before fixation with 4% paraformaldehyde in PBS at room temperature. The remaining procedures are identical to those described above, under "HEK 293T cell stimulation, imaging, and data analysis for calcium-dependent protease cleavage."

HEK 293T cell imaging for comparison of original and evolved LOV domains (Fig. 2d). HEK 293T cells were cultured on glass coverslips pre-treated with human fibronectin (50 µg/mL fibronectin (Millipore) for >10 min at 37 °C before cell plating). HEK cells for characterization of eLOV were transfected with the following plasmids:

- Plasmid P16 from **Supplementary Table 1**, 50 ng/well
- Plasmid P7 from **Supplementary Table 1**, 15 ng/well
- Plasmid P9 from **Supplementary Table 1**, 15 ng/well

Plasmids were combined with 10 µL DMEM and 0.8 µL PEI max, and transfection was carried out as described above under "HEK 293T cell culture and transfection." HEK cells for characterization of the original LOV were transfected with the following plasmids in an analogous manner:

- Plasmid P11 from **Supplementary Table 1**, 50 ng/well
- Plasmid P7 from **Supplementary Table 1**, 15 ng/well
- Plasmid P9 from **Supplementary Table 1**, 15 ng/well

18 h post-transfection, HEK 293T cells were subjected to four different conditions (**Fig. 2d**). Procedures for high-calcium, low-calcium, light, and dark conditions were identical to those described above under "HEK 293T cell stimulation, imaging, and data analysis for light- and calcium-dependent protease cleavage." After immunostaining, cells were imaged at 40× magnification on a Zeiss AxioObserver inverted confocal microscope as described above.

AAV virus supernatant production. AAV virus supernatant was used for neuron culture experiments. To generate viruses, HEK 293T cells were transfected at 60–90%. For each well of HEK cells in a 6-well plate, we combined 0.35 µg viral DNA (plasmid P24, P26, or P28 from **Supplementary Table 1**), 0.29 µg AAV1 serotype plasmid (plasmid P39 in **Supplementary Table 1**), 0.29 µg AAV2 serotype plasmid (plasmid P40 in **Supplementary Table 1**), and 0.7 µg helper plasmid pDF6 (plasmid P41 in **Supplementary Table 1**) with 80 µL serum-free DMEM and 8 µL PEI max. The solution was incubated for 15 min at room temperature, and then 2 mL DMEM supplemented with 10% FBS was added and mixed. Media was aspirated from the HEK 293T cells in the 6-well plate and the 2 mL DNA mix was added gently on the side of the well to the cells. HEK 293T cells were incubated for 48 h at 37 °C and then the supernatant (containing secreted AAV virus) was collected and filtered through a 0.45-µm syringe filter (VWR). AAV virus was aliquotted into sterile Eppendorf tubes (0.5 mL/tube), flash frozen in liquid nitrogen and stored at −80 °C. For production of AAV viruses in T25 flasks, we scaled up by a factor of 2.5; for T75 flasks, we scaled up by a factor of 7.5.

Concentrated AAV virus production. Concentrated AAV virus was prepared for *in vivo* use as described previously[39]. Three T150 flasks of HEK 293T cells with fewer than ten passages were transfected at 80% confluence. For each T150 flask, we combined 5.2 µg vector of interest (e.g., plasmid P24, P26, or P28 from **Supplementary Table 1**), 4.35 µg each of AAV1 and AAV2 serotype plasmids (plasmids P39 and P40 from **Supplementary Table 1**), and 10.4 µg pDF6 adenovirus helper plasmid (plasmid P41 from **Supplementary Table 1**) with 130 µL PEI in 500 µL of serum-free DMEM for 10 min at room temperature. The media in the T150 flask was then removed by aspiration and replaced with 30 mL of complete growth media plus the DNA mixture. HEK293T cells were incubated for 48 h at 37 °C and then the cell pellet was pooled together and collected by centrifugation at 800*g* at room temperature for 10 min. The pellet was resuspended in 20 mL of TBS solution (150 mM NaCl, 20 mM Tris, pH = 8.0). Freshly made 10% sodium deoxycholate (Sigma-Aldrich) in H_2O was added to the resuspended cells to a final concentration of 0.5% and benzonase nuclease (Sigma-Aldrich) was added to a final concentration of 50 units per mL. The solution was incubated at 37 °C for 1 h and then cleared by centrifugation at 3,000*g* for 15 min. The supernatant was loaded using a peristaltic pump (Gilson MP4) at 1 mL/min flow rate onto a HiTrap heparin column (GE healthcare Life Sciences) that was pre-equilibrated with 10 mL of TBS. The column was washed with 20 mL of 100 mM NaCl, 20 mM Tris, pH = 8.0, using the peristaltic pump, followed by washing with 1 mL of 200 mM NaCl, 20 mM Tris, pH = 8.0 and 1 mL of 300 mM NaCl, 20 mM Tris, pH = 8.0 using a 5 mL syringe. The virus was eluted using 5 mL syringes with 1.5 mL of 400 mM NaCl, 20 mM Tris, pH = 8.0; 3.0 mL of 450 mM NaCl, 20 mM Tris, pH = 8.0 and 1.5 mL of 500 mM NaCl, 20 mM Tris, pH = 8.0. The eluted virus was concentrated using Amicon Ultra 15 mL centrifugal units with a 100,000 molecular weight cut off at 2,000× g for 2 min, to a final volume of 500 µL. Then 1 mL sterile DPBS was added to the filter unit and the column was centrifuged again until the virus volume was ~100 µL. The concentrated

AAV virus was divided into 10 µL aliquots in low-stick microcentrifuge tubes (Westnet, Cat# 07-200-183) and stored at −80 °C.

Concentrated AAV virus titration by qPCR. AAV virus (2 µL) was incubated with 1 µL DNase I (NEB, 2 units/µL) in a total volume of 40 µL at 37 °C for 30 min and then deactivated at 75 °C for 15 min. 5 µL of the DNase-treated solution was incubated with 1 µL proteinase K (Thermo Fisher Scientific, 20 mg/mL) in a total volume of 20 µL at 50 °C for 30 min, and then proteinase K was deactivated at 98 °C for 10 min. A 2 µL sample from the proteinase K reaction was used for qPCR analysis.

For each qPCR reaction, 5 µL of SYBR Green master mix (2×) was mixed with 0.3 µM forward primer and 0.3 µM reverse primer (sequences below), 2 µL of proteinase K-treated viral solution from above, and ddH_2O to a final volume of 10 µL per reaction.

Primers for recognition of synapsin promoter (used for AAVs prepared from plasmids P24, P26 and P38 in **Supplementary Table 1**):

Syn-forward: 5′-GGGTGCCTACCTGACGAC

Syn-reverse: 5′-GTGCTGAAGCTGGCAGTG

Primers for recognition of WPRE (used for AAVs prepared from plasmids P28 in **Supplementary Table 1**):

WPRE-forward: 5′-CTGTTGGGCACTGACAATTC

WPRE-reverse: 5′-AGAATCCAGGTGGCAACATA

We prepared standard curves using purified and linearized AAV DNA plasmid (containing both synapsin and WPRE, 5,549 bp) and each viral sample was calculated in reference to the standard curve.

To illustrate:

Number of DNA molecules in 2 ng of linearized standard DNA = $(2 \times 10^{-9}$ g/(5,549 base pair (bp) × 650 Daltons/bp)) × 6.23×10^{23}/mole

if the C_t value of a viral sample matches the C_t value for 2 ng of linearized DNA, then the number of DNA molecules in that qPCR reactions = $(2 \times 10^{-9}$ g/(5,549 bp × 650 Daltons/bp)) × 6.23×10^{23}/mole

Since the final qPCR reactions are only using 2 µL out of the 20 µL proteinase K reaction, and only 5 µL out of the 40 µL DNase I reaction (with 2 µL concentrated AAV virus) was added to the proteinase K reaction, the number of DNA molecules in 1 µL of the original concentrated virus can be derived as the following by adjusting the dilution factors:

$(2 \times 10^{-9}$ g/(5,549 bp × 650 Daltons/bp)) × 6.23×10^{23}/mole × (20 µL/2 µL) × (40 µL/5 µL)/2 µL virus

Note that we multiply final values by 2 because the linearized AAV DNA plasmids are double stranded whereas AAV virus genomic DNA is single-stranded.

Calculated titers for the purified AAV viruses used for the mouse experiments (described below):

- AAV for synapsin-BFP: 10×10^9 viral particle/µL (vp/µL); concentration injected in vivo was 0.5×10^9 vp/µL
- AAV for synapsin-TM-linker-NaV1.6-M2-eLOV-TEVcs-FLAG-tTA-VP16 (FLARE TF component): 28×10^9 vp/µL; concentration injected in vivo was 1.4×10^9 vp/µL
- AAV for synapsin-CaM-V5-TEVp (FLARE protease component): 1.2×10^9 vp/µL; concentration injected in vivo was 0.3×10^9 vp/µL
- AAV for TRE-ChrimsonR-mCherry: 15×10^9 vp/µL; concentration injected in vivo was 1.5×10^9 vp/µL

Rat cortical neuron culture. Cortical neurons were harvested from rat embryos euthanized at embryonic day 18 and plated in 24-well plates as previously described[40], but without glass cover slips. We noticed that neurons grow better and more homogeneously without cover slips. At DIV4, 300 µL media was removed from each well and replaced with 500 µL complete neurobasal media (neurobasal supplemented with 2% (v/v) B27 supplement (Life Technologies), 1% (v/v) Glutamax (Life Technologies), and 1% (v/v) penicillin-streptomycin (VWR, 5,000 units/ml of penicillin and 5,000 µg/mL streptomycin), supplemented with 10 µM 5-fluorodexoyuridine (FUDR, Sigma-Aldrich) to inhibit glial cell growth. Subsequently, approximately 30% of the media in each well was replaced with fresh complete neurobasal media every 3 d. Neurons were maintained at 37 °C under 5% CO_2.

Viral transduction of cortical neuron cultures and stimulation via media change. A mixture of AAV viruses, harvested from HEK 293T supernatant as described above, was added to cultured neurons between DIV10 and DIV15 and incubated for 2 d at 37 °C before 30% of the media in the well was replaced with fresh complete neurobasal media. Typical viral supernatant quantities used were 50 µL of each viral component, added in combination to each well of a 24-well plate dish, already containing 1,500 µL of complete neurobasal media.

After viral transduction, neurons were grown in the dark, wrapped in aluminum foil, and all subsequent manipulations were performed in a dark room with red light illumination to prevent unwanted activation of the LOV domain. Six days post-transduction, neurons were subjected to four conditions: light + high Ca^{2+}; light + low Ca^{2+}; dark + high Ca^{2+}; and dark + low Ca^{2+}. To elevate cytosolic calcium, either 50% or 90% of the media in the well was replaced with fresh complete neurobasal media (whether to change 50% or 90% of the media depends on the health and confluence of the neurons; 50% media change is generally preferred because 90% media change can be too harsh and may produce broken neuronal processes). After this treatment (2–15 min), the saved old culture media was returned to the wells, because we found that this improved the health of the neurons. For the low-calcium condition, neurons were not treated (no media change). For light stimulation, neurons in a 24-well plate were placed on top of the custom-built LED light box described above ("HEK 293T cell stimulation, imaging, and data analysis for light- and calcium-dependent protease cleavage") and irradiated with 467-nm blue light at 60 mW/cm^2 and 10–33% duty cycle. We found that 10% duty cycle (0.5 second of light every 5 s) is sufficient for LOV uncaging. For the dark condition, neurons were wrapped in aluminum foil.

After these treatments, neurons were grown for an additional 16–24 h at 37 °C before fixation with room temperature paraformaldehyde fixative (4% paraformaldehyde, 60 mM PIPES, 25 mM HEPES, 10 mM EGTA, 2 mM $MgCl_2$, 0.12 M sucrose, pH 7.3) for 15 min.

Immunostaining of fixed neurons and imaging. Fixed neurons were permeabilized by incubation with cold methanol at −20 °C for 5 min, washed with PBS twice and then blocked with 2% BSA in PBS at room temperature for 1 h. Neurons were immunostained using mouse-anti-V5 antibody (1:2,000 dilution, Invitrogen) and rabbit-anti-VP16 antibody (1:2,000 dilution, Abcam) in a 2% BSA solution in PBS for 1 h at room temperature with gentle rocking, followed by washing twice with PBS. The neurons were then incubated with anti-mouse-Alexa Flour 488 antibody (1:1,000 dilution, Life Technologies) and anti-rabbit-Alexa Flour 647 antibody (1:1,000 dilution, Life Technologies) in a 2% BSA solution in PBS for 30 min at room temperature with gentle rocking. After washing two times with PBS, the neurons were directly imaged in their 48-well plates using a 10× air objective on a Zeiss AxioObserver inverted confocal microscope. Eight to ten fields of view were collected for each condition.

Analysis of neuron culture imaging data. For each field of view, a mask was created to encompass regions with positive anti-V5 immunofluorescence staining. In these masked regions, the mean mCherry fluorescence intensity was calculated, and background was subtracted (mean mCherry intensity in a V5-negative region). These mean mCherry intensity values were calculated individually for 8–10 fields of view per condition, and plotted in a dot plot. Mean of the means shown as horizontal bars in **Figure 4b** and **4g**. In **Figure 4e** and **Supplementary Figure 9**, errors defined as s.e.m., STD/Sqrt(# of fields of view).

GCaMP5f lentivirus preparation. HEK 293T cells were transfected at 60–90% confluence. For a T25 flask, 2.5 µg GCaMP5f viral DNA (plasmid 42 in **Supplementary Table 1**), 0.25 µg pVSVG (plasmid 43 in **Supplementary Table 1**), and 2.25 µg delta8.9 lentiviral helper plasmid (plasmid 44 in **Supplementary Table 1**) were combined with 200 µL serum-free DMEM and 30 µL PEI max, and incubated for 15 min at room temperature. Then 5 mL DMEM supplemented with 10% FBS was added and mixed. Media was aspirated from the HEK 293T cells and the 5 mL DNA mix was added gently to the cells. HEK 293T cells were incubated for 48 h at 37 °C and then the supernatant (containing secreted lentivirus) was collected and filtered through a 0.45-µm syringe filter (VWR). GCaMP5f lentivirus was divided into aliquots in 0.5 mL sterile Eppendorf tubes, flash frozen in liquid nitrogen, and stored at −80 °C.

doi:10.1038/nbt.3909

GCaMP5f imaging in cultured cortical neurons. DIV14 cortical rat neurons plated in a 24-well plate were infected with lentivirus expressing GCaMP5f. After 5 d of expression, time-lapse imaging was performed before or after replacement of half the media volume with fresh media of identical composition (neurobasal supplemented with 2% (v/v) B27 supplement (Life Technologies), 1% (v/v) Glutamax (Life Technologies) and 1% (v/v) penicillin-streptomycin (VWR, 5,000 units/ml of penicillin and 5,000 µg/mL streptomycin). Imaging was on a confocal microscope using a 10× air objective at room temperature.

Electrical stimulation of cultured neurons infected with GCaMP5. Neurons were infected with 50 µL GCaMP5f lentivirus (HEK cell supernatant) at DIV12, and 30% of the media was replaced with fresh complete neurobasal media 2 d later, at DIV14. Six days post-transduction, at DIV18, electrical stimulation was performed. A Master 8 device (AMPI) was used to induce trains of electric stimuli; a stimulator isolator unit (Warner Instrument, SIU-102b) was used to provide constant current output ranging from 10–100 mA. Platinum iridium alloy (70:30) wire from Alfa-Aesar was folded into a pair of rectangles (0.7 cm × 1.5 cm) and placed right above the neurons on the edge of the well to act as electrodes. Time-lapse images of GCaMP5f fluorescence were acquired with a 10× air objective on a Zeiss AxioObserver inverted confocal microscope while electric stimulation was delivered. We found that 40 mA was the minimum current required to obtain robust GCaMP5f activation. To achieve reliable neuronal activation, 48 mA was used for electric stimulation. To optimize the duration of the stimulus, 0.1, 0.2, 0.5, 1, and 5 ms were tested; a minimum of 1 ms is required. 1 ms and 5 ms did not produce different results; hence, to minimize damage to neurons, we used 1-ms long pulses. We found that GCaMP5f activation with five pulses of 1-ms 20 Hz stimulation was better than one pulse of 5-ms stimulation at 48 mA.

Electric stimulation of neurons transduced with FLARE AAV viruses. At DIV12, cultured neurons were transduced with a mixture of three AAV viruses: P24, P26, and P27 from **Supplementary Table 1**. Total volume of three viruses added to each well was 150 µL. Six days post-transduction, at DIV18, neurons were either irradiated with light (467 nm, 60 mW/cm^2, 10% duty cycle (500 ms on per 5 sec) or kept in the dark when electrical stimulation was performed. A Master 8 device (AMPI) was used to induce trains of electric stimuli; a stimulator isolator unit (Warner Instrument, SIU-102b) was used to provide constant current output ranging from 10–100 mA. Platinum iridium alloy (70:30) wire from Alfa-Aesar was folded into a pair of rectangles (0.7 cm × 1.5 cm) and placed right above the neurons on the edge of the well to act as electrodes.

We used 3-second trains, each consists of 32 1-ms 48 mA pulses at 20 Hz, lasting for a total of 4, 8, or 15 min. Prior to treating FLARE-expressing neurons, we first checked the equipment and protocol on neurons expressing GCaMP5f. We note that electrical stimulation did not give as robust a FLARE turn-on as mechanical stimulation (media change), because the latter produces sustained high Ca^{2+}, whereas the former gives transient Ca^{2+} spikes.

DAB staining of APEX-expressing neurons. Cultured rat cortical neurons were infected at DIV13 with AAV viruses encoding FLARE components: TRE-Citrine-APEX2 (**Supplementary Table 1**, plasmid P38); TM(NRX)-Nav1.6-CaMbp-eLOV-TEVcs-tTA-VP16 (**Supplementary Table 1**, plasmid P24); and CaM-TEVp (**Supplementary Table 1**, plasmid P26). At DIV18, neurons were incubated in the dark or exposed to blue light for 10 min (467 nm, 10% duty cycle, 60 mW/cm^2). Activity stimulation was via 90% media change. 18 h later, neurons were fixed with paraformaldehyde fixative (4% paraformaldehyde, 60 mM PIPES, 25 mM HEPES, 10 mM EGTA, 2 mM $MgCl_2$, 0.12 M sucrose, pH = 7.3) at room temperature for 15 min and washed with cold PBS twice. Then ice-cold 0.5 mg/mL DAB (3,3′-diaminobenzidine) with 0.03% H_2O_2 in PBS was added to the fixed cells, and allowed to sit for 5 min. The DAB polymerization reaction was quenched by washing with PBS two times. Then cells were imaged by DIC.

Reactivation of ChrimsonR in neuron culture (Fig. 4b). Cultured neurons were transduced with FLARE AAV viruses (50 µL of each virus generated from plasmids P24, P26, and P28, **Supplementary Table 1**) and 40 µL GCaMP5f lentivirus added per well of a 24-well plate at DIV13 and incubated at 37 °C with 5% CO_2. At DIV15, 30% of the media from each well was replaced with fresh complete neurobasal media and the neurons were kept in the dark (wrapped in alumina foil) to prevent uncaging of LOV domain (room light can activate LOV domain). The neurons were stimulated at DIV19 at 37 °C with home-built LED light box (467 nm, 60 mW/cm^2, 10% duty cycle (500 ms on per 5 sec)) and electrical stimulation (3 second trains consisting of 32 1-ms 48 mA pulses at 20 Hz for 15 min, see section "Electric stimulation of neurons transduced with FLARE AAV viruses"). The neurons were immediately wrapped in aluminum foil after stimulation and incubated at 37 °C. The neurons were kept in the same old media throughout this process. 18 h later, live neurons in the 24-well plate were imaged with 10× air objective in the confocal microscope at room temperature. ChrimsonR was activated by 568-nm laser (50 mW, 800 ms, 60 mW/cm^2) delivered via the microscope objective every 5 s, as GCaMP5f fluorescence was recorded by (100 ms exposure every 500 ms).

Virus infusion in mice. Adult wild-type male C57BL/6 mice ~8 weeks old (Jackson Laboratory, Bar Harbor, ME) were used for all experiments. All procedures were performed in accordance with guidelines from the NIH and with approval from the MIT Committee on Animal Care (CAC). All surgeries were conducted under aseptic conditions using a digital small-animal stereotaxic instrument (David Kopf Instruments, Tujunga, CA). Mice were anaesthetized with isoflurane (5% for induction, 1.5–2.0% after) in the stereotaxic frame for the entire surgery and their body temperature was maintained using a heating pad. The motor cortex was targeted using the following coordinates from bregma: +1.78 mm AP, 1.5 mm ML, and −1.75 mm DV. The 4 AAV viruses indicated in **Figure 4c** were injected bilaterally using a 10-µL microsyringe with a beveled 33 gauge microinjection needle (nanofil; WPI, Sarasota, FL). Quantities of each virus injected indicated in the Methods section "Concentrated AAV virus titration by qPCR". 1,000 nL of the viral suspensions at a rate of 150 nL/min was infused using a microsyringe pump (UMP3; WPI, Sarasota, FL) and its controller (Micro4; WPI, Sarasota, FL). After each injection the needle was raised 100 µM for an additional 10 min to allow for viral diffusion at the injection site and then slowly withdrawn. In one hemisphere an optic fiber (300 µm core, 0.37 NA) (Thorlabs, Newton, NJ, USA) held in a 1.25-mm ferrule (Precision Fiber Products, Milpitas, CA, USA) was implanted 0.5 mm above the injection site. The optic fiber was held in place using a layer of adhesive cement (C&B metabond; Parkell, Edgewood, NY) followed by a layer of cranioplastic cement (Ortho-Jet; Lang, Wheeling, IL, USA).

Stimulation in mice. Light stimulation was performed 7 d following viral injection. The optic-fiber implants were connected to a 473-nm diode-pumped solid state (DPSS) laser (OEM Laser Systems, Draper, UT, USA). A Master-8 pulse stimulator (A.M.P.I., Jerusalem, Israel) was used to deliver 0.5 mW of 473-nm light: 2-s pulses every 4 s, for 30 min total. For anesthetized experiments, the mice received isoflurane anesthesia (5% for induction, 2–2.5% after) 15 min prior to receiving light and remained under anesthesia for an additional 30 min following light administration. For wheel running experiments, 1 d before the experiment, animals were pre-exposed to the running wheel (Flying Saucer Exercise Wheel for Small Pets, Ware Manufacturing) for 1 h in their home cage. The following day animals were placed on the running wheel.

Brain slice preparation. Animals were euthanized 24 h after receiving stimulation by being deeply anesthetized with sodium pentobarbital (200 mg/kg; intraperitoneal) and transcardially perfused with 10 mL of Ringer's solution followed by 10 mL of cold 4% PFA dissolved in 1× PBS. The excised brains were held in a 4% PFA solution for at least 24 h before being transferred to a 30% sucrose solution in 1× PBS. The brains were then sectioned into 50 µm slices using a sliding microtome (HM420; Thermo Fischer Scientific, Waltham, MA, USA) before being mounted on glass microscope slides, and cover-slipped using PVA mounting medium with DABCO (Sigma-Aldrich, St. Louis, MO, USA).

Confocal microscopy and analysis of mouse brain slices (Supplementary Fig. 12). Confocal imaging was performed with a Zeiss AxioObserver inverted confocal microscope with 10× air objective, outfitted with a Yokogawa spinning

disk confocal head, a Quad-band notch dichroic mirror (405/488/568/647), and 405 (diode), 491 (DPSS), 561 (DPSS) and 640-nm (diode) lasers (all 50 mW). The following laser excitation sources and filter sets were used: BFP (405 laser excitation, 445/40-nm emission) and mCherry (561 laser excitation, 617/73 emission). Acquisition times were 200 ms for BFP and 50 ms for mCherry. All images were collected and processed using SlideBook (Intelligent Imaging Innovations). One field of view was imaged from each brain hemisphere of each section where the mCherry signal was highest, or where BFP signal was highest in cases where mCherry was not observed. If no BFP was observed, no image was taken. To quantify the mCherry signal in each image, a mask was created to capture the mCherry-positive region; a minimum size of 16 pixels was used to define the mask. The mCherry sum intensity within each mask was calculated. For background correction, an area outside of the mCherry region was selected.

For analysis, seven consecutive brain sections were selected per animal. We selected the seven sections with the brightest mCherry signal in the middle of the sequence (the rationale is that the brightest brain slice is closest to the injection site). Animals with no or low BFP signal were omitted due to the possibility of injection or infection failure.

Ex vivo electrophysiology. Mice were deeply anesthetized with sodium pentobarbital (200 mg/kg; intraperitoneal) 24 h following blue light stimulation. They were then transcardially perfused with 20 mL ice-cold ACSF (composition: 87 mM NaCl, 2.5 mM KCl, 1.3 mM NaH_2PO_4, 7 mM $MgCl_2$, 25 mM $NaHCO_3$, 75 mM sucrose, 5 mM ascorbate, 0.5 mM $CaCl_2$, osmolarity 322-325 mOsm, pH = 7.25-7.30) saturated with carbogen gas (95% oxygen, 5% carbon dioxide). The brain was rapidly removed and 300 µm coronal sections containing the motor cortex were prepared on a vibrating-blade microtome (Leica VT1000S, Leica Microsystems, Germany). Slices were maintained in a holding chamber containing ACSF (composition: 126 mM NaCl, 2.5 mM KCl; 1.25 mM NaH_2PO_4*H_20, 1 mM $MgCl_2$*$6H_2O$, 26 mM $NaHCO_3$, 10 mM glucose, 2.4 mM $CaCl_2$*$2H_2O$, osmolarity 299-301 mOsm; pH 7.30-7.35) saturated with carbogen gas at approximately 32 °C for at least 60 min before recording. Brain slices were transferred to the recording chamber and continually perfused at a rate of 2 mL/min using a peristaltic pump (MINIPULS 3; Gilson, USA) with ACSF saturated with carbogen gas at approximately 32 °C. Neurons were visualized through a 40× water-immersion objective on an upright microscope (Scientifica, UK) equipped with infra-red (IR) differential interference contrast (DIC) optics and a Q-imaging Retiga Exi camera (Q Imaging, Canada). Cortical neurons expressing mCherry were identified by brief fluorescence illumination (Lumen 200; Prior Scientific, USA) through a Texas Red filter set (exciter D560/40x, emitter D630/60m).

Electrodes for whole-cell patch-clamp electrophysiology were fabricated from thin-walled borosilicate glass capillary tubing on a P-97 puller (Sutter Instrument, Novato, CA) and had resistances of 5–7 MΩ when filled with internal solution (composition: 125 mM potassium gluconate, 10 mM NaCl, 20 mM HEPES, 3 mM MgATP, and 0.1 % neurobiotin, osmolarity 287 mOsm; pH = 7.30). Recorded signals were amplified using a Multiclamp 700B amplifier (Molecular Devices, CA, USA), low-pass filtered at 1 kHz, digitized at 10 kHz using a Digidata 1550 (Molecular Devices, CA, USA), and acquired with Clampex 10.4 software (Molecular Devices, CA, USA). To monitor cell health, capacitance, series resistance, and input resistance were frequently measured during recordings. ChrimsonR was activated by 5-ms pulses of 589-nm light (irradiance ~28.28 mW/mm^2 at the fiber tip) generated by a 589-nm diode-pumped solid state (DPSS) laser (OEM Laser Systems, Draper, UT) and controlled using a Master-8 pulse stimulator (A.M.P.I., Jerusalem, Israel). Neurons were recorded in current-clamp mode, and light was delivered at 1, 10, and 20 Hz through an optic fiber resting on the brain slice, approximately 0.5 mm from the recorded neuron. Opsin expression was confirmed by observing a constant inward current response to a 1-s light pulse delivered while recording in voltage-clamp mode.

Following recording, brain slices were fixed in 4% paraformaldehyde (PFA) overnight and then washed with PBS (4 × 10 min). For immunohistochemistry, slices were blocked in PBS containing 5% (v/v) normal donkey serum (NDS) and 0.3% Triton for 1 h at room temperature, then incubated with CF633-conjugated streptavidin (1:1,000; Biotum, USA) in PBS containing 3% (v/v) NDS and 0.3% Triton for 2 h at room temperature. Slices were subsequently washed in PBS (4 × 10 min) before mounting on glass slides and coverslipped using polyvinyl alcohol mounting medium with DABCO (PVA-DABCO).

Confocal microscopy of brain slices. Fluorescent images in **Figure 4d**,**f** were obtained using a confocal laser scanning microscope (Olympus FV1000, Olympus, Center Valley, PA, USA) with FluoView software (Olympus, Center Valley, PA, USA) under a 10×/0.40 NA dry objective or a 40×/1.30 NA oil immersion objective.

Photostimulation device for cultured HEK cells and neurons. *In vitro* light stimulation of cultured HEK cells and neurons was performed with a custom-built light box, as described previously[36]. All electronic elements were mounted on a custom-printed circuit board (ExpressPCB). Blue LEDs with peaks at 467 nm (L1-0-B5TH30-1, Ledsupply) were arrayed in groups of three aligned with the wells of a Corning 24-well plate. A DynaOhm driver (Luxdrive dyna-Ohm 4006-025) was used to regulate LED current flow. LED array was controlled by TTL (Fairchild semiconductor PN2222BU-ND) via an Arduino UNO microcontroller board (782-A000073). An 80-mm tall spacer was used surrounding the LED lights to provide support for the 24-well plates. Light output was measured from a distance 100 mm above the array by laser power meter (Coherent Field MAXII-TO). Fans (Evercoll 50 × 15 mm fan, EC5015H12C) were mounted on one wall of the spacer for ventilation.

Arduino control scripts for the custom-made photostimulation device.

```
int led1_pin = 2;
int led2_pin = 3;
int led3_pin = 4;
int led4_pin = 5;
int led5_pin = 6;
int led6_pin = 7;
int uniform_brightness = 280;
int led1_brightness = 1*uniform_brightness/2;
int led2_brightness = 1*uniform_brightness/2;
int led3_brightness = 1*uniform_brightness/2;
int led4_brightness = 1*uniform_brightness/2;
int led5_brightness = 1*uniform_brightness/2;
int led6_brightness = 1*uniform_brightness/2;
unsigned long uniform_stim_time = 500; //'on' time in msec
unsigned long led1_stim_time = uniform_stim_time;
unsigned long led2_stim_time = uniform_stim_time;
unsigned long led3_stim_time = uniform_stim_time;
unsigned long led4_stim_time = uniform_stim_time;//uniform_stim_time;
unsigned long led5_stim_time = uniform_stim_time;
unsigned long led6_stim_time = uniform_stim_time;
unsigned long uniform_off_time = 4500; //periodic time in msec
unsigned long led1_off_time = uniform_off_time;
unsigned long led2_off_time = uniform_off_time;
unsigned long led3_off_time = uniform_off_time;
unsigned long led4_off_time = uniform_off_time;
unsigned long led5_off_time = uniform_off_time;
unsigned long led6_off_time = uniform_off_time;
unsigned long currentMillis = 0;
unsigned long led1_last_change = 0;
unsigned long led2_last_change = 0;
unsigned long led3_last_change = 0;
unsigned long led4_last_change = 0;
unsigned long led5_last_change = 0;
unsigned long led6_last_change = 0;
int led1_state = HIGH;
int led2_state = HIGH;
int led3_state = HIGH;
int led4_state = HIGH;
int led5_state = HIGH;
int led6_state = HIGH;
unsigned long led1_timer = 0;
unsigned long led2_timer = 0;
unsigned long led3_timer = 0;
```


doi:10.1038/nbt.3909

```
unsigned long led4_timer = 0;
unsigned long led5_timer = 0;
unsigned long led6_timer = 0;
void setup() {
  // put your setup code here, to run once:
  pinMode(led1_pin, OUTPUT);
  pinMode(led2_pin, OUTPUT);
  pinMode(led3_pin, OUTPUT);
  pinMode(led4_pin, OUTPUT);
  pinMode(led5_pin, OUTPUT);
  pinMode(led6_pin, OUTPUT);
  analogWrite(led1_pin, led1_brightness);
  analogWrite(led2_pin, led2_brightness);
  analogWrite(led3_pin, led3_brightness);
  analogWrite(led4_pin, led4_brightness);
  analogWrite(led5_pin, led5_brightness);
  analogWrite(led6_pin, led6_brightness);
}
void loop() {
  currentMillis = millis();
  led1_timer = currentMillis - led1_last_change;
  if (led1_state == HIGH){
    if (led1_timer >= led1_stim_time){
      analogWrite(led1_pin, 0);
      led1_state = LOW;
      led1_last_change = currentMillis;
      }
  }
  else{ //led1 state is off
    if (led1_timer >= led1_off_time){
      analogWrite(led1_pin, led1_brightness);
      led1_state = HIGH;
      led1_last_change = currentMillis;
      }
    }
  led2_timer = currentMillis - led2_last_change;
  if (led2_state == HIGH){
    if (led2_timer >= led2_stim_time){
      analogWrite(led2_pin, 0);
      led2_state = LOW;
      led2_last_change = currentMillis;
      }
    }
  else{ //led2 state is off
    if (led2_timer >= led2_off_time){
      analogWrite(led2_pin, led2_brightness);
      led2_state = HIGH;
      led2_last_change = currentMillis;
    }
  }
  led3_timer = currentMillis - led3_last_change;
  if (led3_state == HIGH){
    if (led3_timer >= led3_stim_time){
      analogWrite(led3_pin, 0);
      led3_state = LOW;
      led3_last_change = currentMillis;
    }
  }
  else{ //led3 state is off
    if (led3_timer >= led3_off_time){
    analogWrite(led3_pin, led3_brightness);
      led3_state = HIGH;
      led3_last_change = currentMillis;
    }
  }
  led4_timer = currentMillis - led4_last_change;
  if (led4_state == HIGH){
    if (led4_timer >= led4_stim_time){
    analogWrite(led4_pin, 0);
      led4_state = LOW;
      led4_last_change = currentMillis;
    }
  }
  else{ //led4 state is off
    if (led4_timer >= led4_off_time){
      analogWrite(led4_pin, led4_brightness);
      led4_state = HIGH;
      led4_last_change = currentMillis;
    }
  }
  led5_timer = currentMillis - led5_last_change;
    if (led5_state == HIGH){
      if (led5_timer >= led5_stim_time){
      analogWrite(led5_pin, 0);
      led5_state = LOW;
      led5_last_change = currentMillis;
    }
  }
  else{ //led5 state is off
    if (led5_timer >= led5_off_time){
      analogWrite(led5_pin, led5_brightness);
      led5_state = HIGH;
      led5_last_change = currentMillis;
    }
  }
  led6_timer = currentMillis - led6_last_change;
    if (led6_state == HIGH){
      if (led6_timer >= led6_stim_time){
      analogWrite(led6_pin, 0);
      led6_state = LOW;
      led6_last_change = currentMillis;
    }
  }
  else{ //led6 state is off
    if (led6_timer >= led6_off_time){
      analogWrite(led6_pin, led6_brightness);
      led6_state = HIGH;
      led6_last_change = currentMillis;
      }
    }
  }
```

Data availability. DNA plasmids encoding final FLARE have been deposited to Addgene.

36. Chao, G. *et al.* Isolating and engineering human antibodies using yeast surface display. *Nat. Protoc.* **1**, 755–768 (2006).
37. Zayner, J.P., Antoniou, C., French, A.R., Hause, R.J. Jr. & Sosnick, T.R. Investigating models of protein function and allostery with a widespread mutational analysis of a light-activated protein. *Biophys. J.* **105**, 1027–1036 (2013).
38. Zayner, J.P., Antoniou, C. & Sosnick, T.R. The amino-terminal helix modulates light-activated conformational changes in AsLOV2. *J. Mol. Biol.* **419**, 61–74 (2012).
39. Konermann, S. *et al.* Optical control of mammalian endogenous transcription and epigenetic states. *Nature* **500**, 472–476 (2013).
40. Loh, K.H. *et al.* Proteomic analysis of unbounded cellular compartments: synaptic clefts. *Cell* **166**, 1295–1307.e21 (2016).